4. Baccarani M, Guilhot F, Larson RA, O'Brien SG, Druker BJ. Outcomes by cytogenetic and molecular response at 12 and 18 months of imatinib in patients with newly diagnosed chronic myeloid leukemia (CML) in chronic phase (CP) in the IRIS Trial. Blood 2006;108:2138.
5. Marin D, Milojkovic D, Olavarria E, Khorashad JS, de Lavallade H, Reid AG, et al. European LeukemiaNet criteria for failure or sub-optimal response reliably identify patients with CML in early chronic phase treated with imatinib whose eventual outcome is poor. Blood 2008;112: 4437–4444.
6. Stelzer GT, Shults KE, Loken MR. CD45 gating for routine flow cytometric analysis of human bone marrow specimens. Ann N Y Acad Sci 1993;677:265–280.
7. Borowitz MJ, Guenther KL, Shults KE, Stelzer GT. Immunophenotyping of acute leukemia by flow cytometric analysis. Use of CD45 and right-angle light scatter to gate on leukemic blasts in three-color analysis. Am J Clin Pathol 1993;100:534–540.
8. Branford S, Hughes TP, Rudzki Z. Monitoring chronic myeloid leukaemia therapy by real-time quantitative PCR in blood is a reliable alternative to bone marrow cytogenetics. Br J Haematol 1999;107:587–599.
9. Thiele J, Kvasnicka HM, Titius BR, Parpert U, Nebel R, Zankovich R, et al. Histological features of prognostic significance in CML-an immunohistochemical and morphometric study (multivariate regression analysis) on trephine biopsies of the bone marrow. Ann Hematol 1993;66:291–302.
10. Thiele J, Kvasnicka HM, Schmitt-Graeff A, Zirbes TK, Birnbaum F, Kressmann C, et al. Bone marrow features and clinical findings in chronic myeloid leukemia – a comparative, multicenter, immunohistological and morphometric study on 614 patients. Leuk Lymphoma 2000;36:295–308.
11. Lamba A, Dey P, Kumari S, Marwaha N. Prognostic significance of the histomorphometric features of bone marrow trephine biopsies in patients with chronic myeloid leukemia. Anal Quant Cytol Histol 2007;29:370–376.
12. Valent P, Agis H, Sperr W, Sillaber C, Horny HP. Diagnostic and prognostic value of new biochemical and immunohistochemical parameters in chronic myeloid leukemia. Leuk Lymphoma 2008;49:635–658.
13. Baccarani M, Saglio G, Goldman J, Hochhaus A, Simonsson B, Appelbaum F, et al. Evolving concepts in the management of chronic myeloid leukemia: recommendations from an expert panel on behalf of the European LeukemiaNet. Blood 2006;108:1809–1820.
14. Picard S, Titier K, Etienne G, Teilhet E, Ducint D, Bernard MA, et al. Trough imatinib plasma levels are associated with both cytogenetic and molecular responses to standard-dose imatinib in chronic myeloid leukemia. Blood 2007;109:3496–3499.
15. Larson RA, Druker BJ, Guilhot F, O'Brien SG, Riviere GJ, Krahnke T, et al. Imatinib pharmacokinetics and its correlation with response and safety in chronic-phase chronic myeloid leukemia: a subanalysis of the IRIS study. Blood 2008;111:4022–4028.

THE JOURNAL OF GENE MEDICINE
J Gene Med 2008; **10**: 368–374.
Published online 21 January 2008 in Wiley InterScience (www.interscience.wiley.com) **DOI:** 10.1002/jgm.1166

RESEARCH ARTICLE

Adeno-associated virus vector-mediated systemic interleukin-10 expression ameliorates hypertensive organ damage in Dahl salt-sensitive rats

Mutsuko Nonaka-Sarukawa[1,2]
Takashi Okada[1]
Takayuki Ito[1,2]*
Keiji Yamamoto[2]
Toru Yoshioka[3]
Tatsuya Nomoto[1]
Yukihiro Hojo[2]
Masahisa Shimpo[2]
Masashi Urabe[1]
Hiroaki Mizukami[1]
Akihiro Kume[1]
Uichi Ikeda[3]
Kazuyuki Shimada[2]
Keiya Ozawa[1]*

[1]*Division of Genetic Therapeutics, Jichi Medical University, Japan*

[2]*Division of Cardiovascular Medicine, Jichi Medical University, Japan*

[3]*Department of Organ Regeneration, Shinshu University Graduate School of Medicine, Japan*

*Correspondence to: Takayuki Ito and Keiya Ozawa, Division of Genetic Therapeutics, Centre for Molecular Medicine, Jichi Medical University, 3311-1 Yakushiji, Shimotsuke-shi, Tochigi 329-0498, Japan.
E-mail: titou@jichi.ac.jp and kozawa@jichi.ac.jp

Received: 5 October 2007
Revised: 26 November 2007
Accepted: 11 December 2007

Abstract

Background Inflammation plays an important role in the pathogenesis of hypertension and hypertensive organ damage. Interleukin (IL)-10, a pleiotropic anti-inflammatory cytokine, exerts vasculoprotective effects in many animal models. In the present study, we examined the preventive effects of adeno-associated virus (AAV) vector-mediated sustained IL-10 expression against hypertensive heart disease and renal dysfunction in Dahl salt-sensitive rats.

Methods We injected the rats intramuscularly with an AAV type 1-based vector encoding rat IL-10 or enhanced green fluorescent protein (EGFP) at 5 weeks of age; subsequently, the rats were fed a high-sodium diet from 6 weeks of age.

Results Sustained IL-10 expression significantly improved survival rate of Dahl salt-sensitive rats compared with EGFP expression (62.5% versus 0%, $p < 0.001$); it also caused 26.0% reduction in systolic blood pressure at 15 weeks ($p < 0.0001$). Echocardiography exhibited a 22.0% reduction in hypertrophy ($p < 0.0001$) and a 26.3% improvement in fractional shortening ($p < 0.0001$) of the rat left ventricle in the IL-10 group compared to the EGFP group. IL-10 expression also caused a 21.7% decrease in the heart weight/body weight index and cardiac atrial natriuretic peptide levels. Histopathological studies revealed that IL-10 decreased inflammatory cell infiltration, fibrosis, and transforming growth factor-β_1 levels in the failing heart. Furthermore, IL-10 expression significantly reduced urine protein excretion with increased glomerular filtration rates.

Conclusions This is the first study to demonstrate that the anti-inflammatory cytokine IL-10 has a significant anti-hypertensive effect. AAV vector-mediated IL-10 expression potentially prevents the progression of refractory hypertension and hypertensive organ damage in humans. Copyright © 2008 John Wiley & Sons, Ltd.

Keywords AAV vector; gene therapy; hypertension; inflammation; interleukin-10

Introduction

Inflammation plays an important role in the pathogenesis of hypertension and hypertensive organ damage. Congestive heart failure (CHF) is a crucial life-threatening sequalae of hypertensive organ damage, and

its severity is closely related with the serum tumor necrosis factor (TNF) levels [1,2]. Recent studies have demonstrated the marked anti-hypertensive and renoprotective effects of an immunosuppressant *in vivo* [3,4]. Although these observations suggest a therapeutic potential of anti-inflammatory molecules, anti-TNF antibody treatments (e.g. infliximab and etanercept) have failed to improve the survival of CHF patients partly because of their cytokine-inducing effects and cytotoxicity [5,6].

Interleukin (IL)-10 is a pleiotropic cytokine produced by monocytes/macrophages and type 2 helper T cells. It regulates inflammatory and immune reactions by inhibiting macrophage activation, T-cell proliferation, and the production of proinflammatory cytokines such as TNF-α [7]. IL-10 also enhances endothelial nitric oxide synthase expression [8] and inhibits vascular smooth muscle cell proliferation [9,10]. Previous studies have demonstrated the therapeutic effects of IL-10 on CHF models resulting from acute viral or autoimmune myocarditis [11,12]. However, no studies have examined the effects of IL-10 on chronic CHF resulting from hypertensive heart disease that occurs far more frequently than acute myocarditis. In the present study, we examined the effects of IL-10 using Dahl salt-sensitive (DS) rats that present with severe hypertension and chronic CHF when fed a salt-rich diet [13].

We employed an adeno-associated virus (AAV) type 1-based vector in order to sustain serum levels of IL-10 because it has a short biological half-life. AAV vectors permit long-term transgene expression with minimal inflammatory and immune responses [14]. If the intramuscular injection of the AAV serotype 1 vector carrying the IL-10 gene (AAV1-IL-10) produces sufficient amount of IL-10 in skeletal myocytes, then IL-10 should be secreted into the systemic circulation [10]. We examined the preventive effects of IL-10 on chronic CHF progression in DS rats, focusing on its effects on survival, hypertension, pathological cardiac remodelling and renal function.

Materials and methods

AAV vector production

Rat IL-10 was cloned from rat splenocyte cDNA by the polymerase chain reaction (PCR) using the primers: 5′-GCACGAGAGCCACAACGCA-3′ (upstream) and 5′-GATTTGAGTACGATCCATTTATTCAAAACGAGGAT-3′ (downstream) [10]. To achieve efficient transduction of the skeletal muscles, we developed a recombinant AAV type 1-based vector encoding rat IL-10 (AAV1-IL-10) or enhanced green fluorescence protein (EGFP, AAV1-EGFP) controlled by the modified chicken β-actin promoter with the cytomegalovirus immediate–early enhancer and by the woodchuck hepatitis virus post-transcriptional regulatory element [pBS II SK (+) WPRE-B11, provided by Dr Thomas Hope, University of Illinois, Chicago, IL, USA]. The AAV vectors were prepared by the previously described three-plasmid transfection adenovirus-free protocol modified by the use of the active gassing system [15,16]. Briefly, 60% confluent human embryonic kidney 293 cells were co-transfected with the proviral transgene plasmid, the AAV-1 chimeric helper plasmid p1RepCap (provided by Dr James M. Wilson, University of Pennsylvania, Philadelphia, PA, USA), and the adenoviral helper plasmid pAdeno (provided by Avigen, Inc., Alamada, CA, USA). The crude viral lysate was purified by two rounds of two-tier CsCl centrifugation [14]. The viral stock titer was determined by dot blot hybridization with plasmid standards.

Animal experiment protocols

All animal studies were performed in accordance with the guidelines issued by the committee on animal research and approved by the ethics committee of Jichi Medical University. For histopathological and physiological studies (Protocol 1; Figure 1), we divided the male DS rats (Japan SLC, Shizuoka, Japan) into the following three groups:

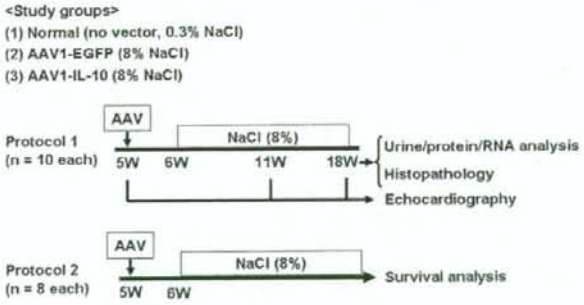

Figure 1. Study protocols. The male DS rats were divided into the three groups: (1) normal group, (2) EGFP group, and (3) IL-10 group. The rats without normal group were injected with AAV1 vectors at 5 weeks of age. The rats in the normal group were fed a low-sodium diet (containing 0.3% NaCl), whereas those in the EGFP or IL-10 group were fed a high-sodium diet (containing 8% NaCl) from 6 weeks of age

IL-10, EGFP and normal ($n = 10$, respectively). AAV1-IL-10 or AAV1-EGFP [1×10^{12} genome copies (g.c.)/body] was injected bilaterally into the anterior tibial muscles of the 5-week-old rats in the IL-10 or EGFP groups, respectively. From 6 weeks onwards, these rats were fed a high-sodium diet (containing 8% NaCl). DS rats in the normal group were fed a low-sodium diet (containing 0.3% NaCl). Systolic blood pressure (SBP) was measured every 2 weeks by the tail-cuff method using a manometer tachometer (MK-1030; Muromachi Kikai Co., Ltd, Tokyo, Japan). During the acclimatization period (3–5 weeks), training for blood pressure measurements was performed three times a week. The mean of the three measurements following a 10-min rest at 37 °C was used in the calculations. Blood was collected from the tail vein at 5,11 and 18 weeks; the sera and plasma were stored at −80 °C. At 18 weeks, the rats were sacrificed by administering an overdose of isoflurane, and their hearts and lungs were harvested and weighed. The tissues were immediately frozen in liquid nitrogen and stored at −80 °C to obtain proteins and RNA for the subsequent analysis. For survival analysis (Protocol 2; Figure 1), the rats were randomly divided into three groups ($n = 8$ each). Those in the IL-10 or EGFP group were injected at 5 weeks of age with the AAV1-IL-10 or AAV1-EGFP (1×10^{11} g.c./body), respectively, and this was followed by a high-sodium diet from 6 weeks of age. By contrast, those in the normal group were fed a low-sodium diet.

Echocardiography

Transthoracic two-dimensional echocardiography was performed at 5, 11 and 18 weeks of age using a 13- MHz transducer (ProSound SSD-α5; Aloka Co., Ltd, Tokyo, Japan). The internal diameter in end-diastole or end-systole of the left ventricle (LVDd or LVDs, respectively) or the posterior wall thickness (PWT) of the left ventricle (LV) in end-diastole was measured by M-mode tracing at the papillary muscle level. The relative wall thickness (RWT) or the percentage fractional shortening (%FS) of LV was calculated according to the formula: RWT = $2 \times$ PWT/LVDd, %FS = (LVDd − LVDs)/LVDd $\times$ 100 (%).

Cytokine measurements

At 18 weeks, protein samples were prepared by homogenizing the frozen heart tissues in a lysis buffer [10 mmol/l Tris-HCl (pH 8.0), 0.2% NP40, 1 mmol/l ethylenediaminetetraacetic acid] containing the protease inhibitor cocktail Complete Mini (Roche Diagnostics, Mannheim, Germany). After centrifugation of the homogenates or serum samples, the supernatants were used for measurement. The serum IL-10 and the tissue transforming growth factor (TGF)-β_1 concentrations were measured by enzyme-linked immunosorbent assay (ELISA) (Amersham PharmaciaBiotech, Bucks, UK; BioSource International, Inc., Camarillo, CA, USA; R&D Systems Inc., Minneapolis, MN, USA). The tissue cytokine levels were standardized using the total protein concentrations estimated by the BCA Protein Assay Kit (Pierce, Rockford, IL, USA).

Quantitative reverse transcriptase (RT)-PCR

At 18 weeks, total RNA was extracted from the heart by using RNAzol B (Tel-Test, Inc., Friendswood, TX, USA) and reverse-transcribed into double-stranded cDNA by using the Superscript Preamplification System (Invitrogen, Carlsbad, CA, USA) with the T7-dT primer (5′-GGCCAGTGAATTGTAATACGACTCACTATAGGGA-GGCGGTTTTTTTTTTTTTTTTTTTTTTT-3′). To estimate the atrial natriuretic protein (ANP) mRNA levels, quantitative PCR analysis was conducted using the ABI Prism 7900 Sequence Detection System (Applied Biosystems, Foster City, CA, USA). The GAPDH mRNA was quantified for normalization. The oligonucleotide primers used were: for GADPH, 5′-CAGCAATGCAT CCTGCAC-3′ (upstream) and 5′-GAGTTGCTGTTGAAGTCACAGG-3′ (downstream) [17]; for ANP, 5′-GGTAGGATTGACAGGATTGGAGCC-3′ (upstream) and 5′-ACATCGATCGTGATAGATGAAGAC-3′ (downstream) [18]. Quantitative values were obtained from the threshold cycle (C_t) number that indicates exponential amplification of a PCR product.

Histopathology

At 18 weeks of age, the anesthetized rats were perfused with 50 ml of saline, followed by 100 ml of cold 4% paraformaldehyde in 0.1 mol/l phosphate buffer (pH 7.4). The hearts were fixed in the same fixative and finally embedded in paraffin. For evaluation of light microscopic findings, we stained sections (3 μm thick) with hematoxylin and eosin (H&E) or the Azan–Mallory stain using the standard methods.

Statistical analysis

The data were assessed using the StatView, version 5.0 (Statview, Abacus Concepts, Berkeley, CA, USA). Differences in the values at specific stages between the groups were assessed by one-way analysis of variance combined with Fisher's test. $p < 0.05$ was considered statistically significant. Survival curves were analysed by the Kaplan–Meier method and compared using log-rank tests.

Results

Pro-survival effect of systemic IL-10 in DS rats

Compared to the control EGFP transduction, IL-10 transduction significantly improved survival rates in DS

rats fed a high-sodium diet ($p < 0.001$, Figure 2). After 13 weeks of the gene delivery, serum IL-10 concentrations significantly increased in the IL-10-transduced rats compared to the normal untreated rats or control EGFP-transduced rats (986.6 ± 278.5 pg/ml versus <3 or 20.8 ± 18.1 pg/ml, $p < 0.001$, respectively; Figure 3). At this time point, the EGFP transduction generated a slight but significant increase of endogenous IL-10 levels compared to control ($p < 0.01$).

Anti-hypertensive effects of IL-10

SBP gradually increased in the EGFP group, resulting in levels of 184 ± 7 mmHg at 15 weeks of age (Figure 4). At 9 weeks (i.e. after 4 weeks of the vector injection), SBP in the IL-10 group (151 ± 7 mmHg) was significantly lower

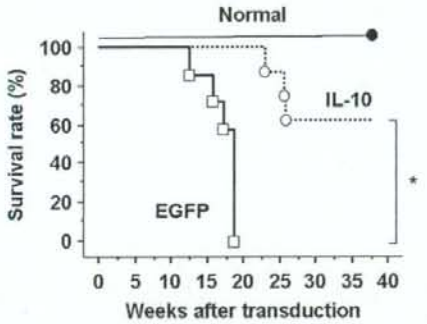

Figure 2. The pro-survival effects of IL-10 in DS rats. The 5-week-old rats were intramuscularly injected with AAV1-IL-10 or AAV1-EGFP at 1×10^{11} g.c./body. Kaplan–Meier survival analysis was performed. Closed circle, normal group; open circles, IL-10 group; open squares, EGFP group ($n = 8$ each). *$p < 0.001$ versus EGFP group

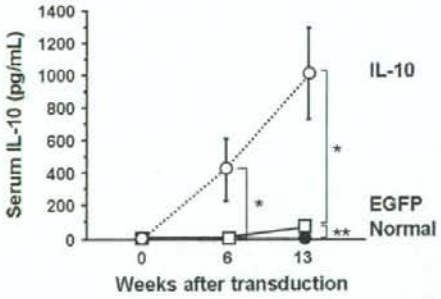

Figure 3. AAV vector-mediated systemic IL-10 expression in DS rats. AAV1-EGFP or AAV1-IL-10, at 1×10^{12} g.c./body, respectively, was injected bilaterally into the anterior tibial muscles of the 5-week-old rats. Serum IL-10 levels were determined periodically by ELISA. The normal group includes DS rats fed a low-sodium diet and not administered the vector injection. The results are presented as means ± SD ($n = 10$ each). *$p < 0.001$, **$p < 0.01$

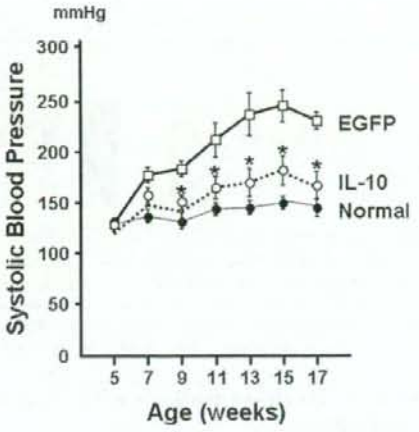

Figure 4. The anti-hypertensive effect of IL-10. Longitudinal tracing of systolic blood pressure evaluated by the tail-cuff method after injecting the AAV vectors in 5-week-old DS rats. Open squares, EGFP group; open circles, IL-10 group; closed circles, normal group ($n = 10$ each). The results are presented as means ± SD. *$p < 0.001$ versus EGFP group

Table 1. Effects of IL-10 on left ventricular hypertrophy and function

	RWT (mm)		%FS (%)	
Age (weeks)	5	11	5	18
Normal	0.46 ± 0.03	0.48 ± 0.02	58.7 ± 3.7	57.2 ± 3.9
EGFP	0.45 ± 0.03	0.63 ± 0.04*	59.8 ± 1.9	32.9 ± 4.4*
IL-10	0.45 ± 0.04	0.49 ± 0.02**	59.4 ± 2.6	59.2 ± 4.6**

M-mode echocardiograms of the LV at the papillary muscle level were traced for analysis. RWT of the LV as an index of LV hypertrophy and %FS as an index of systolic LV function were calculated as described in the Materials and methods. The results are presented as means ± SD ($n = 10$ each). *$p < 0.0001$ versus Normal group, **$p < 0.0001$ versus EGFP group at the same time-point, respectively.

than that in the EGFP group ($p < 0.0001$). The anti-hypertensive effect of IL-10 persisted until the animals were sacrificed at 18 weeks of age.

Effects of IL-10 on left ventricular hypertrophy, function and CHF

Echocardiography exhibited a 22.0% reduction in the RWT of the LV posterior wall at 11 weeks of age ($p < 0.0001$) and a 26.3% improvement in %FS of the LV wall at 18 weeks of age ($p < 0.0001$) in the IL-10 group compared to the EGFP group (Table 1). As compared to EGFP expression, IL-10 expression caused a 21.7% or 52.7% decrease in the heart or lung weight/body weight index, respectively (all $p < 0.05$; Figures 5a and 5b). Similarly, the cardiac ANP mRNA level significantly increased in the EGFP group compared to the control (46.5 ± 23.8-fold); whereas, IL-10 transduction significantly suppressed this increase (9.28 ± 5.2-fold) compared to control (Figure 5c).

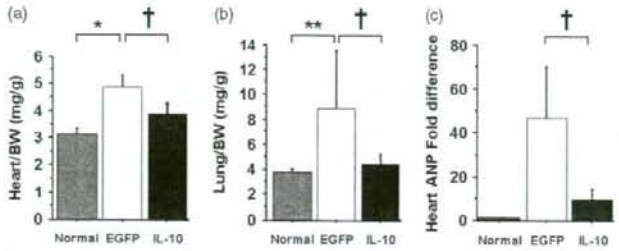

Figure 5. Effects of IL-10 on congestive heart failure. The hearts (a) and lungs (b) of DS rats were harvested and weighed at 18 weeks of age. Data were expressed after normalization using body weight. The cardiac ANP mRNA levels determined by real-time RT-PCR (c). The total RNA was extracted from the heart at 18 weeks of age. The mRNA levels were corrected by using the GAPDH mRNA level of each animal and then normalized to the mean value of the normal group. The results are presented as means ± SD ($n = 10$ each). $^{*}p < 0.01$ versus Normal group, $^{**}p < 0.05$ versus Normal group, $\dagger p < 0.05$ versus EGFP

Effects of IL-10 on pathological cardiac remodelling

H&E staining demonstrated increased interstitial and perivascular cell infiltration in the failing heart of the EGFP-transduced rats (Figure 6a). Azan–Mallory staining demonstrated that interstitial and perivascular fibrosis increased in the EGFP group (Figure 6b). IL-10 transduction inhibited fibrosis and significantly decreased the cardiac TGF-β_1 levels in DS rats compared to the EGFP transduction (64.5 ± 45.3 pg/mg protein versus 197.1 ± 91.9 pg/mg protein, $p < 0.05$; Figure 6c).

Effects of IL-10 on renal function

Compared to control rats, DS rats fed a high-sodium diet exhibited a 68.0% increase in serum creatinine, a 243.0% increase in urine protein levels, and a 49.9% decrease in glomerular filtration rate (all $p < 0.05$; Figure 7). Sustained IL-10 expression reduced these changes by 88.2%, 100% and 45.8%, respectively (all $p < 0.05$).

Discussion

The present study demonstrates that systemic IL-10 expression via the AAV serotype 1 vector prevented the progression of hypertension, CHF and renal dysfunction in DS rats. A single intramuscular injection of AAV1-IL-10 achieved long-term systemic IL-10 expression, leading to the prolonged survival of the rats. The IL-10 transduction not only preserved systolic LV function, but also reduced fibrosis of the LV at the heart failure phase. The anti-hypertensive effect of IL-10 occurred prior to the

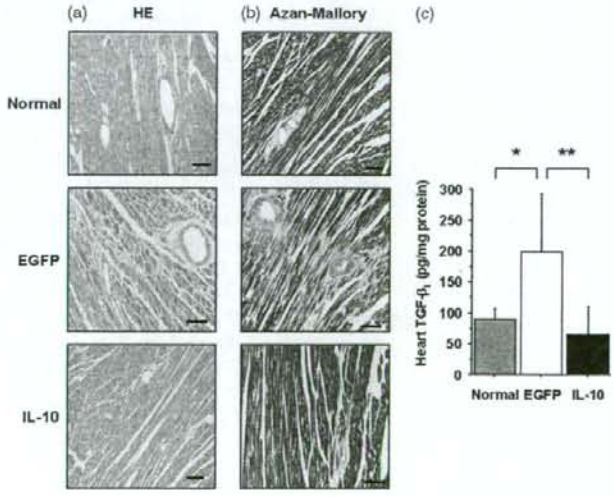

Figure 6. Histopathology and cardiac TGF-β_1 levels of the 18-week-old DS rats. (a) Representative micrographs of the H&E staining. (b) Representative micrographs of Azan–Mallory staining. Magnification, x200; scale bar = 100 μm. (c) TGF-β_1 concentrations in the heart homogenates determined by ELISA. The results are presented as means ± SD ($n = 10$ each). $^{*}p < 0.05$ versus Normal group, $^{**}p < 0.05$ versus EGFP group

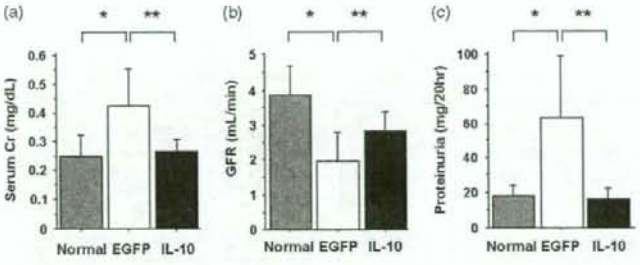

Figure 7. Effects of IL-10 on renal function in DS rats. (a) Serum creatinine (Cr), (b) glomerular filtration rate (GFR) and (c) urine protein levels were determined at 18 weeks of age. The results are presented as means ± SD ($n = 10$ each). *$p < 0.001$ versus Normal group, **$p < 0.05$ versus EGFP group

development of CHF and LVH, suggesting that this effect may largely contribute to amelioration of sodium-induced hypertensive organ damage.

Many studies have suggested the therapeutic potentials of IL-10 for CHF. Serum IL-10 levels decrease in CHF patients [19], and exogenous IL-10 administration retards progression of the disease in many cardiovascular disease models [20]. However, these studies used CHF models in which CHF was a result of acute viral or autoimmune myocarditis, and they examined the short-term IL-10 effects against initial inflammatory responses [11,12]. In the present study, we demonstrated the effects of long-term IL-10 expression against chronic CHF progression, hypertension and inflammatory changes of the cardiac tissue.

We detected a slight but significant increase of endogenous IL-10 levels in the heart failure phase in control DS rats. However, this increase was insufficient to cause beneficial effects. On the other hand, conventional IL-10 therapies based on recombinant drugs or plasmids require frequent administration for sufficient and sustained IL-10 expression. Thus, we used AAV vectors that permit long-term transgene expression *in vivo* [14]. Previously, we demonstrated that a single intramuscular injection of the AAV5-based vector caused systemic IL-10 expression for 1 year [21]. Since AAV1 is more efficient for muscle transduction than AAV2 or AAV5 [22], we used AAV1 as the vector in the present study [23].

A clinical trial using infliximab, a chimeric monoclonal antibody to TNF-α, failed to prolong the survival of CHF patients over the long term [5]. We speculate that the failure might be in part based on an insufficient regulation of the cytokine network, which may be involved in the progression of CHF and other related diseases such as hypertension and renal failure. Recent studies have shown the marked anti-hypertensive effects of an immunosuppressant mycophenolate mofetil (MMF) in DS rats [3,4]. MMF administration also ameliorates renal dysfunction via anti-inflammatory effects. Interestingly, an intramuscular injection of AAV1-IL-10 successfully ameliorated renal function in a rat model after nephrectomy [24]. We also observed that systemic IL-10 expression significantly attenuated hypertension and renal dysfunction, along with a decrease of inflammatory cell infiltration, in the kidney of stroke-prone spontaneously hypertensive rats (T. Nomoto *et al.*, unpublished data). In the present study, we demonstrate that IL-10 gene therapy successfully ameliorated heart failure and renal dysfunction along with a suppression of severe hypertension in DS rats. These observations suggest that anti-inflammatory action of IL-10 may attenuate the target organ damage related to high blood pressure. However, precise mechanism underlying the anti-hypertensive effect of IL-10 require further investigation.

The synthesis of ANP, a cardioprotective hormone predominantly produced by the ventricle, as well as its circulating levels, increases in accordance with the severity of CHF [25,26]. Administration of exogenous ANP ameliorates CHF in clinical settings via its diuretic and vasodilatory effects. In the present study, the cardiac ANP mRNA level significantly decreased in the IL-10 group. These observations suggest that IL-10 ameliorated CHF independently of direct ANP production but inhibited the adaptive increase in ANP levels.

The present study demonstrates that IL-10 expression attenuated pathological cardiac remodelling with reduced expression of TGF-β_1, a hallmark of cardiac fibrosis in DS rats [27]. Expression of monocyte chemoattractant protein (MCP)-1 in the endothelium of intramyocardial arterioles triggers perivascular macrophage accumulation [28]. Macrophage infiltration induces TGF-β_1 production, leading to fibroblast proliferation and extracellular matrix production [29]. Interestingly, a neutralizing antibody against TGF-β inhibits fibroblast activation, resulting in reduced collagen production and subsequent myocardial fibrosis [30]. Previously, we reported that systemic IL-10 expression significantly decreased serum MCP-1 levels, perivascular macrophage infiltration, and pulmonary tissue TGF-β_1 levels *in vivo* [10,21]. These observations suggest that the reduced macrophage-derived TGF-β_1 expression following MCP-1 suppression might be responsible for the anti-remodelling effects of IL-10. However, the direct effects of IL-10 on TGF-β_1 in the pathogenesis of CHF remain unclear.

Epidemiological studies have demonstrated that the increased pro-inflammatory cytokine expression is related to the incidence of pre-hypertension [31]. These results

suggest a possible link between the inflammatory response and the development of hypertension. This is the first study to demonstrate the anti-hypertensive effects of IL-10, which might be a key molecule to explain this relationship. Exploring the mechanisms underlying the effects of IL-10 would provide new molecular targets for refractory hypertension and its sequalae.

In conclusion, the sustained IL-10 expression achieved by the single AAV-IL-10 injection ameliorated CHF and prolonged survival in DS rats. IL-10 expression attenuated salt-sensitive hypertension, LV remodelling and renal dysfunction. These results suggest that our IL-10-based strategy potentially prevents the progression of refractory hypertensive organ damage in humans.

Acknowledgements

We thank Miyoko Mitsu and Takako Takagi for their encouragement and technical support. This work was supported by grants from the Ministry of Health, Labour and Welfare of Japan. This work was also supported by Grants-in-Aid for Scientific Research; a grant from the 21 Century COE program; and High-Tech Research Centre Project for Private Universities, matching fund subsidy, from the Ministry of Education, Culture, Sports, Science and Technology of Japan; and a research award to Jichi Medical School Graduate Student. This work was performed at Jichi Medical University in Shimotuke-shi, Tochigi, Japan.

References

1. Levine B, Kalman J, Mayer L, *et al.* Elevated circulating levels of tumor necrosis factor in severe chronic heart failure. *N Engl J Med* 1990; **323**: 236–241.
2. Vasan RS, Sullivan LM, Roubenoff R, *et al.* Inflammatory markers and risk of heart failure in elderly subjects without prior myocardial infarction: the Framingham Heart Study. *Circulation* 2003; **107**: 1486–1491.
3. Mattson DL, James L, Berdan EA, *et al.* Immune suppression attenuates hypertension and renal disease in the Dahl salt-sensitive rat. *Hypertension* 2006; **48**: 149–156.
4. Tian N, Gu JW, Jordan S, *et al.* Immune suppression prevents renal damage and dysfunction and reduces arterial pressure in salt-sensitive hypertension. *Am J Physiol Heart Circ Physiol* 2007; **292**: H1018–H1025.
5. Chung ES, Packer M, Lo KH, *et al.* Randomized, double-blind, placebo-controlled, pilot trial of infliximab, a chimeric monoclonal antibody to tumor necrosis factor-alpha, in patients with moderate-to-severe heart failure: results of the anti-TNF Therapy Against Congestive Heart Failure (ATTACH) trial. *Circulation* 2003; **107**: 3133–3140.
6. Mann DL, McMurray JJ, Packer M, *et al.* Targeted anticytokine therapy in patients with chronic heart failure: results of the Randomized Etanercept Worldwide Evaluation (RENEWAL). *Circulation* 2004; **109**: 1594–1602.
7. Elenkov IJ, Chrousos GP. Stress hormones, proinflammatory and antiinflammatory cytokines, and autoimmunity. *Ann NY Acad Sci* 2002; **966**: 290–303.
8. Cattaruzza M, Slodowski W, Stojakovic M, *et al.* Interleukin-10 induction of nitric-oxide synthase expression attenuates CD40-mediated interleukin-12 synthesis in human endothelial cells. *J Biol Chem* 2003; **278**: 37874–37880.
9. Selzman CH, McIntyre RC, Jr., Shames BD, *et al.* Interleukin-10 inhibits human vascular smooth muscle proliferation. *J Mol Cell Cardiol* 1998; **30**: 889–896.
10. Ito T, Okada T, Miyashita H, *et al.* Interleukin-10 expression mediated by an adeno-associated virus vector prevents monocrotaline-induced pulmonary arterial hypertension in rats. *Circ Res* 2007; **101**: 734–741.
11. Nishio R, Matsumori A, Shioi T, *et al.* Treatment of experimental viral myocarditis with interleukin-10. *Circulation* 1999; **100**: 1102–1108.
12. Palaniyandi SS, Watanabe K, Ma M, *et al.* Inhibition of mast cells by interleukin-10 gene transfer contributes to protection against acute myocarditis in rats. *Eur J Immunol* 2004; **34**: 3508–3515.
13. Kihara Y, Sasayama S. Transition from compensatory hypertrophy to dilated failing left ventricle in Dahl-Iwai salt-sensitive rats. *Am J Hypertens* 1997; **10**: 78S–82S.
14. Okada T, Shimazaki K, Nomoto T, *et al.* Adeno-associated viral vector-mediated gene therapy of ischemia-induced neuronal death. *Methods Enzymol* 2002; **346**: 378–393.
15. Matsushita T, Elliger S, Elliger C, *et al.* Adeno-associated virus vectors can be efficiently produced without helper virus. *Gene Ther* 1998; **5**: 938–945.
16. Okada T, Nomoto T, Yoshioka T, *et al.* Large-scale production of recombinant viruses by use of a large culture vessel with active gassing. *Hum Gene Ther* 2005; **16**: 1212–1218.
17. Nakahara T, Hashimoto K, Hirano M, *et al.* Acute and chronic effects of alcohol exposure on skeletal muscle c-myc, p53, and Bcl-2 mRNA expression. *Am J Physiol Endocrinol Metab* 2003; **285**: E1273–1281.
18. Ueno S, Ohki R, Hashimoto T, *et al.* DNA microarray analysis of in vivo progression mechanism of heart failure. *Biochem Biophys Res Commun* 2003; **307**: 771–777.
19. Stumpf C, Lehner C, Yilmaz A, *et al.* Decrease of serum levels of the anti-inflammatory cytokine interleukin-10 in patients with advanced chronic heart failure. *Clin Sci (Lond)* 2003; **105**: 45–50.
20. Ito T, Ikeda U. Inflammatory cytokines and cardiovascular disease. *Curr Drug Targets Inflamm Allergy* 2003; **2**: 257–265.
21. Yoshioka T, Okada T, Maeda Y, *et al.* Adeno-associated virus vector-mediated interleukin-10 gene transfer inhibits atherosclerosis in apolipoprotein E-deficient mice. *Gene Ther* 2004; **11**: 1772–1779.
22. Hauck B, Chen L, Xiao W. Generation and characterization of chimeric recombinant AAV vectors. *Mol Ther* 2003; **7**: 419–425.
23. Ito T, Okada T, Mimuro J, *et al.* Adenoassociated virus-mediated prostacyclin synthase expression prevents pulmonary arterial hypertension in rats. *Hypertension* 2007; **50**: 531–536.
24. Mu W, Ouyang X, Agarwal A, *et al.* IL-10 suppresses chemokines, inflammation, and fibrosis in a model of chronic renal disease. *J Am Soc Nephrol* 2005; **16**: 3651–3660.
25. Saito Y, Nakao K, Arai H, *et al.* Augmented expression of atrial natriuretic polypeptide gene in ventricle of human failing heart. *J Clin Invest* 1989; **83**: 298–305.
26. de Boer RA, Henning RH, Suurmeijer AJ, *et al.* Early expression of natriuretic peptides and SERCA in mild heart failure: association with severity of the disease. *Int J Cardiol* 2001; **78**: 5–12.
27. Ichihara S, Obata K, Yamada Y, *et al.* Attenuation of cardiac dysfunction by a PPAR-alpha agonist is associated with down-regulation of redox-regulated transcription factors. *J Mol Cell Cardiol* 2006; **41**: 318–329.
28. Kuwahara F, Kai H, Tokuda K, *et al.* Hypertensive myocardial fibrosis and diastolic dysfunction: another model of inflammation? *Hypertension* 2004; **43**: 739–745.
29. Border WA, Noble NA. Transforming growth factor beta in tissue fibrosis. *N Engl J Med* 1994; **331**: 1286–1292.
30. Kuwahara F, Kai H, Tokuda K, *et al.* Transforming growth factor-beta function blocking prevents myocardial fibrosis and diastolic dysfunction, in pressure-overloaded rats. *Circulation* 2002; **106**: 130–135.
31. Chrysohoou C, Pitsavos C, Panagiotakos DB, *et al.* Association between prehypertension status and inflammatory markers related to atherosclerotic disease: the ATTICA Study. *Am J Hypertens* 2004; **17**: 568–573.

Protection Against Aminoglycoside-induced Ototoxicity by Regulated AAV Vector–mediated GDNF Gene Transfer Into the Cochlea

Yuhe Liu[1,2,3], Takashi Okada[1,4], Kuniko Shimazaki[5], Kianoush Sheykholeslami[6], Tatsuya Nomoto[1], Shin-Ichi Muramatsu[7], Hiroaki Mizukami[1], Akihiro Kume[1], Shuifang Xiao[3], Keiichi Ichimura[2] and Keiya Ozawa[1]

[1]Division of Genetic Therapeutics, Jichi Medical University, Tochigi, Japan; [2]Department of Otolaryngology, Jichi Medical University, Tochigi, Japan; [3]Department of Otolaryngology, Peking University First Hospital, Beijing, China; [4]Department of Molecular Therapy, National Institute of Neuroscience, National Center of Neurology and Psychiatry, Tokyo, Japan; [5]Department of Physiology, Jichi Medical University, Tochigi, Japan; [6]Department of Neurobiology, Northeastern Ohio Universities College of Medicine, Rootstown, Ohio, USA; [7]Division of Neurology, Department of Medicine, Jichi Medical University, Tochigi, Japan

Since standard aminoglycoside treatment progressively causes hearing disturbance with hair cell degeneration, systemic use of the drugs is limited. Adeno-associated virus (AAV)-based vectors have been of great interest because they mediate stable transgene expression in a variety of postmitotic cells with minimal toxicity. In this study, we investigated the effects of regulated AAV1-mediated glial cell line–derived neurotrophic factor (GDNF) expression in the cochlea on aminoglycoside-induced damage. AAV1-based vectors encoding GDNF or vectors encoding GDNF with an rtTA2s-S2 Tet-on regulation system were directly microinjected into the rat cochleae through the round window at 5×10^{10} genome copies/body. Seven days after the virus injection, a dose of 333 mg/kg of kanamycin was subcutaneously given twice daily for 12 consecutive days. GDNF expression in the cochlea was confirmed and successfully modulated by the Tet-on system. Monitoring of the auditory brain stem response revealed an improvement of cochlear function after GDNF transduction over the frequencies tested. Damaged spiral ganglion cells and hair cells were significantly reduced by GDNF expression. Our results suggest that AAV1-mediated expression of GDNF using a regulated expression system in the cochlea is a promising strategy to protect the cochlea from aminoglycoside-induced damage.

Received 12 May 2007; accepted 15 November 2007; published online 8 January 2008. doi:10.1038/sj.mt.6300379

INTRODUCTION

Aminoglycoside antibiotics are frequently used in empiric therapy for serious infections, such as septicemia, complicated intra-abdominal infections, complicated urinary tract infections, and nosocomial respiratory tract infections. However, it is well known that aminoglycosides are associated with severe side effects, such as ototoxicity and nephrotoxicity, which attack the cochlea or vestibule and destroys the auditory and vestibular hair cells that pass information to the auditory nerve.[1] In addition, aminoglycosides predominantly destroy the outer hair cells by ototoxicity. Although the exact mechanism of damage is not well established,[2] aminoglycoside-induced hair cell loss results in a permanent hearing deficit[3] that can progressively occur 6 months to a year after exposure to these drugs. Therefore, the development of a strategy to prevent aminoglycoside-associated ototoxicity before adverse events occur is a critical issue in clinical settings.

The expression of a transgene using viral vectors is a potential approach to introduce neurotrophic factors into the cochlea to prevent and treat aminoglycoside-induced hearing loss. However, most of the currently used vectors, such as adenovirus vectors or herpes simplex virus vectors, have an associated vector-related cytotoxicity.[4,5] Hence, adeno-associated virus (AAV) vectors may be good candidates for gene transfer into the cochlear cells because of their efficient transduction and their safety and potential in long-term expression.[6] We have previously demonstrated that an AAV1-based vector efficiently transduced the inner hair cells, the spiral ganglion cells, and many other types of cells.[7] Therefore, an AAV1-based vector should successfully introduce secretory proteins, such as glial cell line–derived neurotrophic factor (GDNF), into the cochlea to prevent aminoglycoside-induced ototoxicity.

GDNF, a member of the transforming growth factor β family, was initially identified as a survival factor for mid-brain dopaminergic neurons and for a wide range of neuronal populations in the central and peripheral nervous systems.[8–10] Although it is still unclear whether GDNF protects against ototoxicity, sustained infusion of recombinant GDNF protected the cochlear structure and function from noise- and drug-induced damage and stress,[11–18] although its half-life is very short. However, an overdose of GDNF was shown to enhance the sensitivity of the cochleae to insult and

Correspondence: Takashi Okada, Department of Molecular Therapy, National Institute of Neuroscience, National Center of Neurology and Psychiatry, 4-1-1 Ogawa-Higashi, Kodaira, Tokyo 187-8551, Japan. E-mail: t-okada@ncnp.go.jp; Keiya Ozawa, Division of Genetic Therapeutics, Center for Molecular Medicine, Jichi Medical University, 3311-1 Yakushiji, Shimotsuke, Tochigi 329-0498, Japan. E-mail: kozawa@jichi.ac.jp

to destroy cochlear function.[12] Furthermore, it has been reported that testicular tumors are formed in GDNF-overexpressing mice.[19] Therefore, an appropriate regulation system is required to realize the therapeutic benefits of GDNF expression.

Regulated transgene expression has been successfully achieved in various gene therapy experiments using the Tet system.[20–23] Notably, tetracycline derivatives, such as doxycycline (Dox), activate the Tet-on system at doses 100-fold lower than tetracycline. Furthermore, the reverse Tet-responsive transcriptional activator (rtTA) series were improved through the generation of variants called rtTA2s-S2, which showed lower leakiness and better inducibility in HeLa cells and mice.[24,25]

In this study, we describe *in vivo* therapeutic experiments utilizing AAV1 vector–mediated tetracycline-regulated expression of GDNF in cochleae. We demonstrate that AAV1 vector–mediated GDNF expression protects sensory cells in the inner ear from drug-induced degeneration.

RESULTS

Expression and distribution of transgene in the cochlea

AAV1-EGFP or AAV1-GDNF containing either the enhanced humanized green fluorescent protein (*EGFP*) gene or the *GDNF* gene under the control of the CAG (human cytomegalovirus (CMV) immediate-early enhancer and Chicken β-actin promoter) promoter, and the Woodchuck hepatitis virus posttranscriptional regulatory element (WPRE) (**Figure 1a**), was injected into the cochlea. The GDNF protein level in the perilymph was measured by enzyme-linked immunosorbent assay (**Figure 2a**). There was a significant increase in GDNF concentration in the cochlea transduced with AAV1-GDNF. The widespread distribution of the GDNF expression was observed in the cochlea, including the spiral ganglion and the inner hair cells (**Figure 2b**).

To examine the possible transduction of the contralateral ear with the virus diffusion, we analyzed the AAV vector–meditated transgene expression of the rodents with this transduction approach using the optical bioluminescence imaging. Luciferase expression was mainly detected at the injected side of the cochleae (5,370.3 photons/sec/cm^2/sr, **Supplementary Figure S1**). Interestingly, the AAV vector also transduced the contralateral ear (876.8 photons/sec/cm^2/sr), along with the brain (792.9 photons/sec/cm^2/sr). Similar results were obtained with repeated experiments.

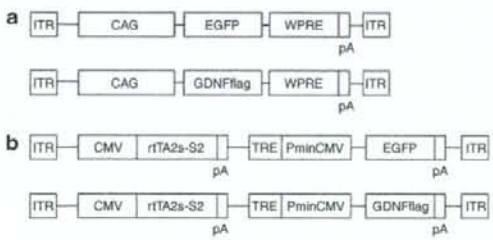

Figure 1 Schematic representation of the viral vectors used in this study. (**a**) An adeno-associated virus 1 (AAV1)-based vector was constructed using the CAG promoter to drive enhanced green fluorescent protein (EGFP) or mouse glial cell line–derived neurotrophic factor (GDNF) with a FLAG tag (GDNFflag). The Woodchuck hepatitis virus posttranscriptional regulatory element (WPRE) was inserted into the 3′ end of the transgene cassette. (**b**) The transactivator rtTA2s-S2 is under the control of the CMV promoter. The minimal CMV promoter (PminCMV) induces transgene expression (EGFP or GDNFflag) in combination with the Tetracycline-responsive element (TRE) and transactivator. CAG, human cytomegalovirus immediate-early enhancer and Chicken β-actin promoter; CMV, cytomegalovirus immediate-early promoter; pA, the simian virus 40 polyadenylation sequences; ITR, inverted terminal repeat from AAV2.

Preservation of the hair cells and spiral ganglion cells in the cochlea

Hair cell loss in the whole-mount cochleae of all the tested rat groups was analyzed by F-actin staining with rhodamine–phalloidin. **Figure 3a** shows a representative dissection through the second turn of the rat cochlea, in which a full complement of hair cells is revealed by F-actin phalloidin staining. In the vehicle-treated control group, outer hair cells in the base and middle turn were drastically lost after kanamycin treatment (**Figure 3b**). In the AAV1-GDNF/kanamycin-treated group, successful protection of the hair cells in the cochlea was observed (**Figure 3c**). In the contralateral cochlea, some of outer hair cells were also protected (**Figure 3d**). The spiral ganglion cell loss in the basal turn of the cochlea was assessed using 4′,6-diamino-2-phenylindole dihydrochloride staining (**Figure 4a** and **b**). Survival of the spiral ganglion cells in the AAV1-GDNF injected cochlea was significantly improved compared to that in the AAV1-EGFP injected cochlea (**Figure 4c**).

Protection of cochlear function by GDNF

Auditory brain stem response (ABR) recordings of the aminoglycoside-treated animals were performed to examine hearing

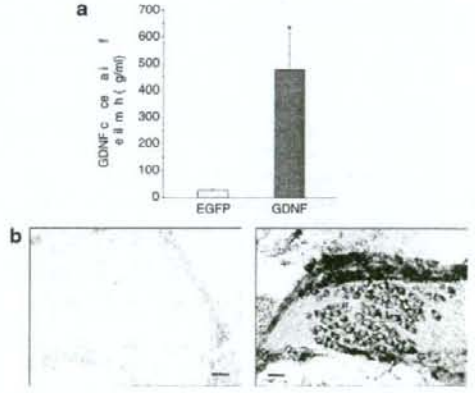

Figure 2 Expression and distribution of transgene in the cochlea. (**a**) Cochlear glial cell line–derived neurotrophic factor (GDNF) expression levels were measured by enzyme-linked immunosorbent assay in the transduced rats. GDNF expression level of the perilymph in the AAV1-GDNF/kanamycin group was significantly higher than that in the control group ($n = 5$, $P < 0.001$). (**b**) Immunohistochemistry was performed to analyze the expression of the GDNFflag in the rat cochlea. The AAV1-EGFP-transduced cochlea was used as a control (left). Cochlear sections were prepared after AAV1-GDNF injection and kanamycin administration. GDNflag expression was detected in the cochlea with an anti-FLAG antibody (right). Scale bar = 25 μm; ×400. AAV1, adeno-associated virus 1; EGFP, enhanced green fluorescent protein.

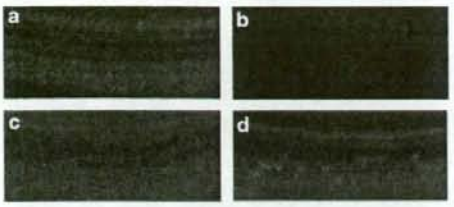

Figure 3 Preservation of the hair cells in the transduced cochlea. Hair cell loss in the cochlea of transduced rats was analyzed by F-actin staining. The dissected samples were dissected from the middle turn of the cochlea. The adeno-asssociated virus 1 (AAV1) vector was injected into the scala tympani of the cochlea prior to 12 days of kanamycin administration. (**a**) The normal cochlea. (**b**) The cochlea from the vehicle-treated ear; the many dark spaces represent the loss of outer hair cells. (**c**) The cochlea from the AAV1-GDNF-transduced ear. (**d**) The cochlea from the contralateral ear of AAV1-GDNF transduced rats. GDNF, glial cell line–derived neurotrophic factor.

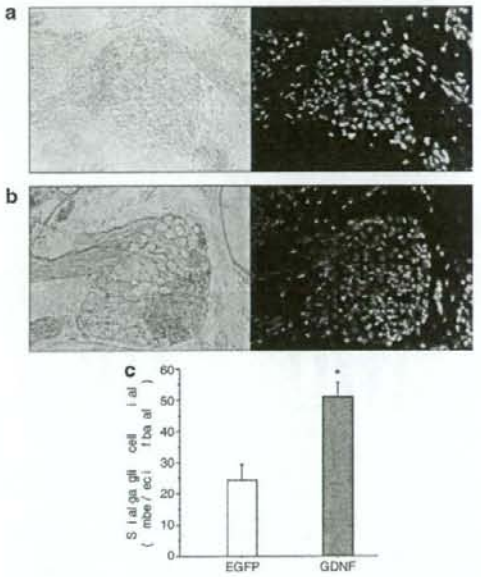

Figure 4 Survival of the spiral ganglion cells in the transduced cochlea. AAV1-GDNF-mediated rescue of the kanamycin-induced damage to the rat spiral ganglion neurons (SGNs): 4′,6-diamino-2-phenylindole dihydrochloride (DAPI) staining was performed on the sections obtained from the rat pretreated with either AAV1-EGFP or AAV1-GDNF, followed by kanamycin injections. (**a**, **b**) Representative photomicrographs of the cryosections showing the basal turn of the cochlear spiral (**a**, AAV1-EGFP; **b**, AAV1-GDNF). (**c**) The number of DAPI-positive large-nucleus cells that exhibited SGN morphology was counted. An asterisk denotes a statistically significant difference between the AAV1-GDNF and AAV1-EGFP-transduced rats (*t*-test, $P < 0.001$). AAV1, adeno-associated virus 1; EGFP, enhanced green fluorescent protein; glial cell line–derived neurotrophic factor.

impairment. At all frequencies tested, both GDNF-transduced and contralateral, untreated ears showed a significant improvement in the threshold shifts compared to the ears transduced with EGFP ($n = 5$, $P < 0.05$) (**Figure 5**). In the EGFP group, there was

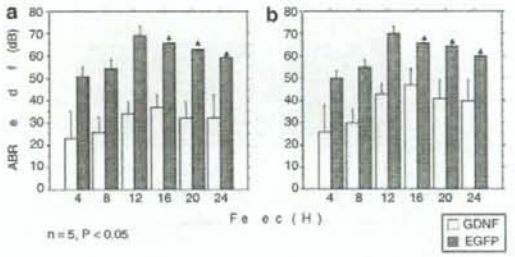

Figure 5 Protection of cochlear function by glial cell line–derived neurotrophic factor GDNF. Auditory brain stem response (ABR) threshold shifts (mean ± SD) of the (**a**) treated and (**b**) untreated ears at each tested frequency in the enhanced green fluorescent protein (EGFP) and GDNF transduced rats. The ABR threshold was measured twice in all the animals. The ears treated with AAV1-GDNF showed a significant improvement in the threshold shifts compared to the ears treated with AAV1-EGFP at all frequencies tested ($n = 5$, $P < 0.05$). Arrows indicate the average ABR thresholds that exceeded the output power of the ABR apparatus. AAV1, adeno-associated virus 1.

no significant difference in the ABR threshold shifts between the transduced and contralateral, untreated cochleae at all frequencies tested. Animals transduced with the AAV1-GDNF demonstrated lower ABR threshold shifts in the injected side compared to the contralateral side (at 12, 16, 20, 24 kHz; $P < 0.05$). These data indicate that both ears were protected even if the AAV1-GDNF was only injected into one ear.

Induced transgene expression

Two hundred and ninety three cells were transduced with the proviral plasmid harboring rtTA2s-S2 and the tetracycline-responsive element (TRE) to express the *EGFP* gene (**Figure 1b**). In the presence of Dox, a significant level of fluorescence was detected, suggesting that the rtTA2s-S2 system could switch on transcription following Dox treatment (**Figure 6a**). In contrast, reporter gene expression in the cultured cells was faint in the absence of Dox, indicating a low basal activity *in vitro*. Western blot analysis of GDNF showed that the transgene was induced in the presence of Dox, while no expression was detected in the absence of Dox (**Figure 6b**).

In vivo induction of GDNF expression and the dose–response to Dox

Enzyme-linked immunosorbent assay analysis of the GDNF expression level in muscle also showed low basal activity and induced expression after Dox treatment (**Figure 6c**). In the absence of Dox, the expression level of GDNF in the AAV2-S2-GDNF group was as low as that in the phosphate-buffered saline and AAV2-*LacZ* groups. On the other hand, significant increases in the GDNF level were observed in the muscle with increasing amounts of Dox, demonstrating that the rtTA2s-S2 system induces gene expression in a dose-dependent manner.

Inducible GDNF expression in the cochlea

Extensive inducible GDNF transgene expression was confirmed by immunohistochemistry using an anti-FLAG-antibody in the AAV1-S2-GDNF/kanamycin group in the presence of Dox (**Figure 7**).

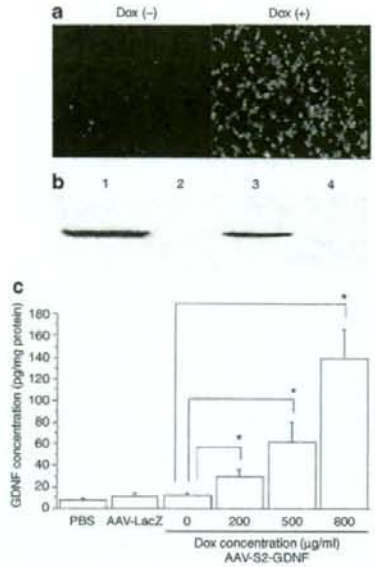

Figure 6 Induction of the transgene expression. (**a**) HEK293 cells were transfected with the proviral plasmid pAAV2-rtTA-S2-TRE-d2EGFP, and the expression of enhanced green fluorescent protein (EGFP) was induced by the doxycycline (Dox) (1 μg/ml). (**b**) Western blot analysis with an anti-FLAG antibody to detect the glial cell line–derived neurotrophic factor (GDNF) expression in the transduced 293 cells with the proviral plasmids. pAAV2-GDNF (lane 1), pAAV2-EGFP (lane 2), pAAV2-rtTA2s-S2-TRE-GDNF with Dox (lane 3), and pAAV2-rtTA2s-S2-TRE-GDNF without Dox (lane 4). (**c**) Dose–response of GDNF in the AAV2-S2-GDNF-injected muscle to the various concentrations of Dox. Mice were injected with phosphate-buffered saline (PBS), AAV2-LacZ, or AAV2-S2-GDNF followed by Dox administered in the drinking water. The mean muscle GDNF concentration in the animals treated with the AAV2-S2-GDNF in the absence of Dox was not significantly different compared to the animals treated with PBS or AAV2-*LacZ* ($P > 0.05$). The GDNF expression levels in the animals transduced with the AAV2-S2-GDNF significantly increased with increasing Dox concentration ($P < 0.05$). AAV1, adeno-associated virus 1.

In contrast, no detectable GDNF expression was observed in the cochlea of the AAV1-S2-GDNF/kanamycin group in the absence of Dox (data not shown).

Protection of cochlear function with induced GDNF expression

To evaluate the adverse effects of the transduction procedure, ABR recordings were performed on kanamycin-free rats after injection of the inducible AAV1-S2-GDNF vectors and Dox administration. At all frequencies tested, no significant increase in the ABR threshold was observed after virus injection (**Figure 8a**). This result indicates that AAV1 vector injection, transgene expression, and Dox administration did not affect the ABR threshold of the experimental rats. Interestingly, even if AAV1-S2-GDNF was injected into the cochlea of one ear, the cochleas of both ears were protected in the presence of Dox. In particular, the ABR threshold shifts were significantly improved in both the AAV1-S2-GDNF-injected cochlea of the kanamycin-treated rats in the presence of Dox (**Figure 8b**)

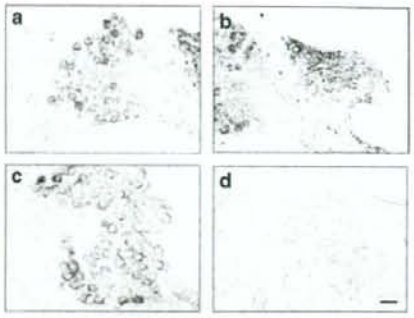

Figure 7 Expression of the GDNFflag in the rat cochlea. (**a**, **b**, **c**) The sections were sampled after the AAV1-S2-GDNF injection into the cochlea in the presence of doxycycline. GDNFflag expression was detected using an anti-FLAG antibody. (**d**) Samples from AAV1-EGFP-inoculated cochlea were analyzed as the negative control. Scale bar = 25 μm; ×400. AAV1, adeno-associated virus 1; GDNF, glial cell line–derived neurotrophic factor; EGFP, enhanced green fluorescent protein.

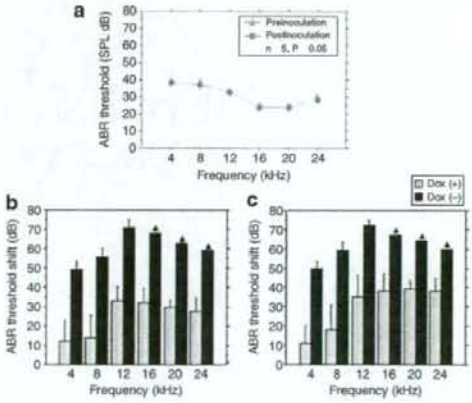

Figure 8 Protection of cochlear function with induced glial cell line–derived neurotrophic factor (GDNF) expression. (**a**) Auditory brain stem response (ABR) thresholds (mean ± SD) at each frequency tested in the AAV1-S2-GDNF-injected rat cochlea in the presence of doxycycline (Dox). No significant difference in the hearing thresholds was observed at each frequency between preinjection and postinjection. SPL, sound pressure level. ABR threshold shifts (mean ± SD) at each tested frequency in the (**b**) transduced or (**c**) nontransduced cochlea with or without Dox. Significant differences in the hearing threshold shifts were observed at each frequency between AAV1-S2-GDNF cochlea in the presence and absence of Dox ($n = 5$, $P < 0.05$). Arrows indicate the average ABR thresholds that exceeded the output power of the ABR apparatus.

and the cochlea of the noninjected contralateral ear (**Figure 8c**). However, the ABR threshold shifts at all frequencies were significantly lower in the treated group (AAV1-S2-GDNF/kanamycin plus Dox) than in the contralateral, untreated ear.

DISCUSSION

In this study, we showed that both sustained and regulated AAV1-mediated GDNF expression protected the cochlear function of rats from aminoglycoside-induced ototoxicity. Indeed, damaged spiral ganglion cells and hair cells were significantly reduced by

regulated GDNF expression. The ABR monitoring revealed that there was no loss of the cochlear function over the frequencies tested after AAV vector injection and Dox treatment. These data suggest that regulated expression of GDNF in the cochlea efficiently preserves the cochlea from kanamycin-induced ototoxicity.

Among the various viral vector systems, the recombinant AAV-mediated gene transduction system offers several important advantages as a tool for direct somatic gene delivery into the cochlea. These include long-term stable expression of therapeutic genes in a wide variety of postmitotic tissues and minimal vector-related cytotoxicity.[26] In our previous report, we demonstrated the effective transduction of mouse cochleae with the AAV1-based vectors.[7] Generally the therapeutic effectiveness depends on an appropriate concentration and the half-life of the molecules. AAV vector–mediated gene transfer is a promising delivery technique to facilitate a long-term and chronic supply of therapeutic proteins that have a short half-life, such as GDNF. Furthermore, when the CAG promoter is used, efficient transduction activity is observed in the cochlear cells including the inner hair cells and spiral ganglion cells.[27,28]

Our data showed that AAV1-GDNF-mediated transduction of the rat cochleae provided significant protection of the cochlea against aminoglycoside-induced damage. This finding is consistent with previous studies that have used adenovirus-mediated GDNF expression[13,15,16] and demonstrates the feasibility of gene therapy with AAV1-based vectors for drug-induced hearing loss. Although the exact mechanism has not yet been elucidated, antioxidant pathways might be involved in the protective function of GDNF in the inner ear.[29] Free-radical formation following exposure to aminoglycoside is considered one of the major mechanisms to explain the aminoglycoside-related hair cell death.[1,30,31] It has been previously shown that GDNF is endogenously synthesized in the inner hair cells and spiral ganglion cells of the cochlea,[32] and the two known GDNF receptors are present in the spiral ganglion.[17,32,33] In the present study, we inoculated the cochlea with the AAV1 vectors via the round window membrane and detected a high level of transgene expression mainly in the inner hair cells and spiral ganglion cells. The AAV1-mediated GDNF expression pattern was similar to that of the endogenous protein; therefore GDNF supplemented *in situ* can play a substantial role in protection. Although the transduction of the *GDNF* gene was not observed in outer hair cells, GDNF levels in the perilymph of the manipulated cochleae was much higher than in the control cochleae. These cells may respond to the secretion of another growth factor that promotes hair cell survival. Upregulation of GDNF in inner hair cells and spiral ganglion cells following noise also support this concept.[34]

Compared to the vehicle controls, increased cochlear cell survival was observed in the contralateral ears of the AAV1-GDNF group, suggesting that the contralateral cochleae in treated rats were also moderately protected. Expression of the transgene was detected in the contralateral cochlea of the rats after injection with 5×10^{10} genome copies of AAV1 per cochlea (data not shown). AAV can diffuse from one ear to the other via the cerebrospinal fluid in rodents.[35] Therefore, secreted GDNF molecules may also diffuse and exert a protective effect in the opposite ear. Alternatively, GDNF might enhance the neuronal activity (either afferent or efferent) of both ears, protecting both the treated and the contralateral cochlear function. Moreover, since infusion of the vectors into the cochlea forces large amounts of the vectors into the cerebrospinal fluid, any functional effect might be associated with the transduction of the brain. In this context, it is of great interest to know whether the otoprotective effect was achieved by the simple diffusion of the transgene product or direct transduction of the cells in the contralateral ear. To answer this question, we analyzed the local expression of the nonsecretory protein marker in the rodents with this transduction approach. Consequently, we feel that the direct transduction of the cells in the contralateral ear might be involved in the neuroprotection.

The present results showed that AAV-mediated delivery of a Tet-on system was able to control transgene expression. This Tet-on system incorporates the mutant transactivator rtTA2s-S2 and the transgene in which messenger RNA transcription is activated in the presence of an inducer, leading to protein expression. As we showed, the inducible expression of GDNF efficiently protected the cochlear structure and function from kanamycin-induced damage. GDNF was overexpressed in the induced state with the rtTA2s-S2 system, whereas GDNF expression was nearly normal in the non-induced state. In our study, cochlear function was significantly protected from aminoglycoside-induced cochlear damage in the presence of Dox. Although intracochlear injections did not affect physiological cochlear function, intramuscular injections of the vectors expressing Dox-dependent activators may elicit a cellular and humoral response against the transactivator in nonhuman primates.[36–38] The use of tissue-specific promoters that restrict transgene expression to nonprofessional antigen-presenting cells, and the use of AAV vectors, may reduce the induction of a specific T-cell response.[39]

Another attractive feature of the Tet-on system is the high safety profile of the inducer. In our study, Dox was orally administered to the rats to induce GDNF expression. Transgene expression levels were dependent on the dose of Dox, and the dose range of this inducer was below the normal bactericidal treatment levels used in similarly sized animals.[40,41] Furthermore, a Dox regimen in mice that is proportional to a clinically accepted dose of the drug in humans causes a significant induction of transgene expression.

Sequences of antibiotic administration and withdrawal to reverse the Dox induction of therapeutic gene expression were demonstrated in previous studies.[25,42] However, the aminoglycoside-induced hearing impairment model is not an appropriate model for adding and removing the Dox diet because the insulting phase is too short to successively induce and repress the Tet-on system. Furthermore, treatment of age-related hearing loss or genetic hearing loss ideally needs long-term gene expression studies to exclude any adverse events associated with the therapeutic genes.

Efficient control of the tetracycline-regulatory system is based on the specificity of the TetR/tetO interaction and the efficiency and safety of its inducers, such as tetracycline or Dox.[43,44] Mutant tTA2s are composed of one TetR and three repeated oligonucleotides of the VP-16-derived minimal activation domain. In the Tet-on system, rtTA2s-S2 showed a high activating ratio because its background expression level was lower than that of other mutants, such as rtTA2s-M2, which despite having a higher activation potential had also a high initial background.[25] By using the mutant transactivator, Urlinger *et al.* demonstrated that stringent regulation of target genes could be achieved over a range of four to five orders of magnitude

in stably transfected HeLa cells.[24] These regulatory systems could be further optimized to offer several potential advantages. The tetracycline-dependent transcriptional silencer allows tight regulation of transgene expression by eliminating baseline leakage.[20,43] Gene regulation mediated by rtTA2s-S2 was substantially tighter when combined with active silencing by the tetracycline-dependent transcriptional silencer in the non-induced state.[41,46]

Our results show that AAV1-mediated gene transfer is a promising gene delivery approach for the inner ear apparatus. To become an efficient and safe therapeutic method, it will be necessary to improve vector technology to achieve long-term transduction in a fail-safe system. We presented data demonstrating successful AAV-mediated transfer and modulation of transgene expression in the cochlea using a modified Tet-on system. In addition to the need for dosage control of neurotrophic factors, the AAV1 and the Tet-on system maybe useful for the regulation of the expression of other therapeutic gene products in the cochlea. Following further improvements, the rAAV-mediated transduction system may be of potential use for cochlear gene therapy applications in humans.

MATERIALS AND METHODS

Construction and preparation of the plasmids. The AAV vector proviral plasmid pAAV2-CAG-EGFP-WPRE (pAAV2-EGFP) contained the *EGFP* gene under the control of the CAG promoter and the WPRE and was flanked by inverted terminal repeats. A *Bam*HI fragment containing the GDNFflag complementary DNA was subcloned into this plasmid to obtain the pAAV2-CAG-GDNF-WPRE (pAAV2-GDNF) cassette.

The pAAV2-CMV-GDNFflag plasmid with the CMV promoter, the first intron of the human growth hormone gene, and the simian virus 40 polyadenylation signal sequence, were inserted between the inverted terminal repeats of the AAV type 2 genome.[47] The transactivator rtTA2s-S2 complementary DNA in the pUHrT61-1 plasmid (BD Biosciences, San Jose, CA) and the TRE in the pTRE-d2EGFP plasmid (BD Biosciences, CA) were subcloned together into the pAAV2-CMV-GDNFflag plasmid to obtain the AAV vector proviral plasmid pAAV2-rtTA2s-S2-TRE-GDNF. A *Sac*II-*Eco*RI fragment containing the d2EGFP complementary DNA from the pTRE-d2EGFP plasmid (BD Biosciences, CA) was subcloned into this plasmid to create the pAAV2-rtTA2s-S2-TRE-EGFP plasmid (see **Supplementary Materials and Methods**).

Recombinant AAV vector production. The AAV1 vectors were produced as previously described by using a 293-cell transfection protocol[24] with the proviral plasmid pAAV2-EGFP, pAAV2-Luciferase,[48] pAAV2-GDNF, pAAV2-rtTA2s-S2-TRE-EGFP, or pAAV2-rtTA2s-S2-TRE-GDNF; the AAV packaging plasmid pAAV1RepCap; and the adenovirus helper plasmid pAdeno5 using an active gassing system.[49] The recombinant AAV2 expressing the *Escherichia coli* β-galactosidase gene under the control of the CMV promoter (AAV2-LacZ) was generated using the proviral plasmid pAAV-LacZ.[50] (see **Supplementary Materials and Methods**).

In vitro *expression of GDNF.* To detect the *in vitro* expression of the GDNFflag fusion protein, 293 cells were transduced with the AAV1-GDNFflag at 1×10^4 vector genome copies/cell. For the detection of the regulated expression, 293 cells were transduced with the AAV proviral plasmid pAAV2-rtTA2s-S2-TRE-d2EGFP or pAAV2-rtTA2s-S2-TRE-GDNF in the presence or absence of 1 μmol/l Dox-HCl (Sigma, St Louis, MO) (see **Supplementary Materials and Methods**).

Surgical procedures and cochlear perfusions. All animal studies were performed in accordance with the guidelines issued by the committee on animal research at Jichi Medical University. Twenty 5-week-old male Sprague–Dawley rats with normal Preyer's reflexes weighing 130–150 g were utilized (CLEA Japan, Tokyo, Japan). Five-week-old male C57BL/6J mice were utilized for optical bioluminescence imaging. The animals were anesthetized with ketamine (50 mg/kg) and xylazine (5 mg/kg). A post-auricular approach was performed to expose the tympanic bony bulla. A small opening (2 mm in diameter) to the tympanic bulla was made by carefully drilling through the bone of the bulla to gain access to the round window membrane. Subsequently, 5 μl of AAV vector solution (AAV1-EGFP, AAV2-Luciferase, or AAV1-GDNF, 5×10^{10} genome copies, $n = 5$ each) was microinjected into the cochlea through the round window for over 10 minutes using a glass micropipette (40 μm in diameter) fitted on a Univentor 801 syringe pump (Serial No. 170182, High Precision Instruments, Univentor Ltd., Malta). The rats were also injected with the AAV1-S2-GDNF in the presence ($n = 5$) or absence ($n = 5$) of Dox. A small plug of muscle was used to seal the cochlea, and the surgical wound was closed in layers and dressed with an antibiotic ointment.

***Transgene expression* in vivo.** The rats were deeply anesthetized and the perilymph was sampled from the inoculated cochlea through the round window. GDNF protein levels were measured using a GDNF Emax ImmunoAssay System (Promega, Madison, WI) according to the manufacturer's instructions. The GDNF expression in the rat cochlea was determined by immunohistochemistry using an anti-FLAG antibody.

AAV2-LacZ or AAV2-S2-GDNF vector (1×10^{10} genome copies) was injected into the quadriceps of the C57BL/6J mice (6 weeks old, CLEA Japan, Tokyo, Japan). The mice were injected with phosphate-buffered saline ($n = 5$) or AAV2-*LacZ* ($n = 5$). Animals treated with various concentrations of Dox were injected with the AAV2-S2-GDNF ($n = 5$ per group). Two weeks after the transduction, animals were deeply anesthetized, and the injected muscle was sampled. The tissue levels of the GDNF protein were measured with an enzyme-linked immunosorbent assay kit (GDNF Emax ImmunoAssay System, Promega, WI), according to the manufacturer's instructions. The levels of GDNF were expressed as pg/mg protein. The assay sensitivity ranged from 16 to 1,000 pg/ml.

Two weeks after the injection of the AAV2-Luciferase, optical bioluminescence imaging was performed using the CCD camera (Xenogen, Alameda, CA). After intraperitoneal injection of reporter substrate D-Luciferin (375 mg/kg body weight), mice were imaged for scans.

Kanamycin administration and ABR assessment. A dose of 333 mg of kanamycin base/kg body weight was obtained by injecting 3 μl/g body weight. Seven days after virus injection, kanamycin was given subcutaneously twice daily for 12 consecutive days. The body weight of the animals was monitored daily to adjust the kanamycin dosages accordingly.

Auditory thresholds were determined by audiometry of evoked ABRs using Tucker-DAVIS Technologies and Scope software (Power Lab; ADInstruments, Coloado Springs, CO). Thresholds were evaluated for each animal prior to the start of the injection procedure and 2 days after the termination of kanamycin treatment. The ABRs were measured as previously described,[7] using a two-way repeated analysis of variance (see **Supplementary Materials and Methods**).

Histological evaluation of the cochlear preservation. Cochlear hair cell loss was determined by F-actin staining. One month after transduction, the presence of the cochlear spiral ganglion neurons was determined by 4′,6-diamino-2-phenylindole dihydrochloride staining to visualize nuclear chromatin. After decalcification, 6 μm mid-modiolus cryosections of the cochleae from each animal were histologically analyzed. The number of spiral ganglion neurons was determined in every third section of the cochlear basal turn from the AAV1-transduced and kanamycin-treated rats (see **Supplementary Materials and Methods**).

Statistical analyses. Results are presented as the means ± SD. Data were statistically analyzed using analysis of variance, paired student's *t*-test (injected versus contralateral sides) or unpaired student's *t*-test (therapy versus control groups) (StatView 5.0 software; SAS Institute, Cary, NC).

ACKNOWLEDGMENTS

The authors thank Avigen, (Alameda, CA) for providing the pAAV-LacZ and pAdeno. We also thank Thomas Hope (Department of Microbiology and Immunology, The University of Illinois at Chicago) for providing pBS II SK+WPRE-B11 and Jun-Ichi Miyazaki (Osaka University Graduate School of Medicine, Osaka, Japan) for pCAGGS. The authors also thank Miyoko Mitsu for her encouragement and technical support. This work was supported in part by grants from the Ministry of Health, Labour and Welfare of Japan (Grants-in-Aid for Scientific Research and grant for 21 Century Centers of Excellence program) and the "High-Tech Research Center" Project for Private Universities (matching fund subsidy, from the Ministry of Education, Culture, Sports, Science, and Technology of Japan). The authors declare no conflict of interest.

SUPPLEMENTARY MATERIAL

Materials and Methods.

Figure S1. Bioluminescence of the transduced cochlea in living mice.

REFERENCES

1. Wu, WJ, Sha, SH and Schacht, J (2002). Recent advances in understanding aminoglycoside ototoxicity and its prevention. *Audiol Neurootol* **7**: 171–174.
2. Hellier, WP, Wagstaff, SA, O'Leary, SJ and Shepherd, RK (2002). Functional and morphological response of the stria vascularis following a sensorineural hearing loss. *Hear Res* **172**: 127–136.
3. Tsue, TT, Oesterle, EC and Rubel, EW (1994). Hair cell regeneration in the inner ear. *Otolaryngol Head Neck Surg* **111**: 281–301.
4. Raphael, Y, Frisancho, JC and Roessler, BJ (1996). Adenoviral-mediated gene transfer into guinea pig cochlear cells *in vivo*. *Neurosci Lett* **207**: 137–141.
5. Ishimoto, S, Kawamoto, K, Kanzaki, S and Raphael, Y (2002). Gene transfer into supporting cells of the organ of Corti. *Hear Res* **173**: 187–197.
6. Okada, T, Nomoto, T, Shimazaki, K, Lijun, W, Lu, Y, Matsushita, T *et al.* (2002). Adeno-associated virus vectors for gene transfer to the brain. *Methods* **28**: 237–247.
7. Liu, Y, Okada, T, Sheykholeslami, K, Shimazaki, K, Nomoto, T, Muramatsu, SI *et al.* (2005). Specific and efficient transduction of cochlear inner hair cells with recombinant adeno-associated virus type 3 vector. *Mol Ther* **12**: 725–733.
8. Lin, LF, Doherty, DH, Lile, JD, Bektesh, S and Collins, F (1993). GDNF: a glial cell line-derived neurotrophic factor for midbrain dopaminergic neurons. *Science* **260**: 1130–1132.
9. Henderson, CE, Phillips, HS, Pollock, RA, Davies, AM, Lemeulle, C, Armanini, M *et al.* (1994). GDNF: a potent survival factor for motoneurons present in peripheral nerve and muscle. *Science* **266**: 1062–1064.
10. Wang, Y, Lin, SZ, Chiou, AL, Williams, LR and Hoffer, BJ (1997). Glial cell line-derived neurotrophic factor protects against ischemia-induced injury in the cerebral cortex. *J Neurosci* **17**: 4341–4348.
11. Keithley, EM, Ma, CL, Ryan, AF, Louis, JC and Magal, E (1998). GDNF protects the cochlea against noise damage. *Neuroreport* **9**: 2183–2187.
12. Shoji, F, Yamasoba, T, Magal, E, Dolan, DF, Altschuler, RA and Miller, JM (2000). Glial cell line-derived neurotrophic factor has a dose dependent influence on noise-induced hearing loss in the guinea pig cochlea. *Hear Res* **142**: 41–55.
13. Suzuki, M, Yagi, M, Brown, JN, Miller, AL, Miller, JM and Raphael, Y (2000). Effect of transgenic GDNF expression on gentamicin-induced cochlear and vestibular toxicity. *Gene Ther* **7**: 1046–1054.
14. Yagi, M, Kanzaki, S, Kawamoto, K, Shin, B, Shah, PP, Magal, E *et al.* (2000). Spiral ganglion neurons are protected from degeneration by GDNF gene therapy. *J Assoc Res Otolaryngol* **1**: 315–325.
15. Hakuba, N, Watabe, K, Hyodo, J, Ohashi, T, Eto, Y, Taniguchi, M *et al.* (2003). Adenovirus-mediated overexpression of a gene prevents hearing loss and progressive inner hair cell loss after transient cochlear ischemia in gerbils. *Gene Ther* **10**: 426–433.
16. Kawamoto, K, Yagi, M, Stover, T, Kanzaki, S and Raphael, Y (2003). Hearing and hair cells are protected by adenoviral gene therapy with TGF-beta1 and GDNF. *Mol Ther* **7**: 484–492.
17. Kuang, R, Hever, G, Zajic, G, Yan, Q, Collins, F, Louis, JC *et al.* (1999). Glial cell line-derived neurotrophic factor. Potential for otoprotection. *Ann NY Acad Sci* **884**: 270–291.
18. Yagi, M, Magal, E, Sheng, Z, Ang, KA and Raphael, Y (1999). Hair cell protection from aminoglycoside ototoxicity by adenovirus-mediated overexpression of glial cell line-derived neurotrophic factor. *Hum Gene Ther* **10**: 813–823.
19. Meng, X, Lindahl, M, Hyvonen, ME, Parvinen, M, de Rooij, DG, Hess, MW *et al.* (2000). Regulation of cell fate decision of undifferentiated spermatogonia by GDNF. *Science* **287**: 1489–1493.
20. Perez, N, Plence, P, Millet, V, Greuet, D, Minot, C, Noel, D *et al.* (2002). Tetracycline transcriptional silencer tightly controls transgene expression after *in vivo* intramuscular electrotransfer: application to interleukin 10 therapy in experimental arthritis. *Hum Gene Ther* **13**: 2161–2172.
21. Regulier, E, Pereira de Almeida, L, Sommer, B, Aebischer, P and Deglon, N (2002). Dose-dependent neuroprotective effect of ciliary neurotrophic factor delivered via tetracycline-regulated lentiviral vectors in the quinolinic acid rat model of Huntington's disease. *Hum Gene Ther* **13**: 1981–1990.
22. Rubinchik, S, Worarattanadharm, J, Yu, H and Dong, JY (2005). New complex Ad vectors incorporating both rtTA and tTS deliver tightly regulated transgene expression both *in vitro* and *in vivo*. *Gene Ther* **12**: 504–511.
23. Pluta, K, Luce, MJ, Bao, L, Agha-Mohammadi, S and Reiser, J (2005). Tight control of transgene expression by lentivirus vectors containing second-generation tetracycline-responsive promoters. *J Gene Med* **7**: 803–817.
24. Urlinger, S, Baron, U, Thellmann, M, Hasan, MT, Bujard, H and Hillen, W (2000). Exploring the sequence space for tetracycline-dependent transcriptional activators: novel mutations yield expanded range and sensitivity. *Proc Natl Acad Sci USA* **97**: 7963–7968.
25. Lamartina, S, Roscilli, G, Rinaudo, CD, Sporeno, E, Silvi, L, Hillen, W *et al.* (2002). Stringent control of gene expression *in vivo* by using novel doxycycline-dependent trans-activators. *Hum Gene Ther* **13**: 199–210.
26. Okada, T, Shimazaki, K, Nomoto, T, Matsushita, T, Mizukami, H, Urabe, M *et al.* (2002). Adeno-associated viral vector-mediated gene therapy of ischemia-induced neuronal death. *Methods Enzymol* **346**: 378–393.
27. Stone, IM, Lurie, DI, Kelley, MW and Poulsen, DJ (2005). Adeno-associated virus-mediated gene transfer to hair cells and support cells of the murine cochlea. *Mol Ther* **11**: 843–848.
28. Liu, Y, Okada, T, Nomoto, T, Ke, X, Kume, A, Ozawa, K *et al.* (2007). Promoter effects of adeno-associated viral vector for transgene expression in the cochlea *in vivo*. *Exp Mol Med* **39**: 170–175.
29. Oppenheim, RW (1997). Related mechanisms of action of growth factors and antioxidants in apoptosis: an overview. *Adv Neurol* **72**: 69–78.
30. Priuska, EM and Schacht, J (1995). Formation of free radicals by gentamicin and iron and evidence for an iron/gentamicin complex. *Biochem Pharmacol* **50**: 1749–1752.
31. Sha, SH and Schacht, J (1999). Stimulation of free radical formation by aminoglycoside antibiotics. *Hear Res* **128**: 112–118.
32. Sanicola, M, Hession, C, Worley, D, Carmillo, P, Ehrenfels, C, Walus, L *et al.* (1997). Glial cell line-derived neurotrophic factor-dependent RET activation can be mediated by two different cell-surface accessory proteins. *Proc Natl Acad Sci USA* **94**: 6238–6243.
33. Ylikoski, J, Pirvola, U, Virkkala, J, Suvanto, P, Liang, XQ, Magal, E *et al.* (1998). Guinea pig auditory neurons are protected by glial cell line-derived growth factor from degeneration after noise trauma. *Hear Res* **124**: 17–26.
34. Nam, YJ, Stover, T, Hartman, SS and Altschuler, RA (2000). Upregulation of glial cell line-derived neurotrophic factor (GDNF) in the rat cochlea following noise. *Hear Res* **146**: 1–6.
35. Kho, ST, Pettis, RM, Mhatre, AN and Lalwani, AK (2000). Safety of adeno-associated virus as cochlear gene transfer vector: analysis of distant spread beyond injected cochleae. *Mol Ther* **2**: 368–373.
36. Favre, D, Blouin, V, Provost, N, Spisek, R, Porrot, F, Bohl, D *et al.* (2002). Lack of an immune response against the tetracycline-dependent transactivator correlates with long-term doxycycline-regulated transgene expression in non-human primates after intramuscular injection of recombinant adeno-associated virus. *J Virol* **76**: 11605–11611.
37. Latta-Mahieu, M, Rolland, M, Caillet, C, Wang, M, Kennel, P, Mahfouz, I *et al.* (2002). Gene transfer of a chimeric trans-activator is immunogenic and results in short-lived transgene expression. *Hum Gene Ther* **13**: 1611–1620.
38. Lena, AM, Giannetti, P, Sporeno, E, Ciliberto, G and Savino, R (2005). Immune responses against tetracycline-dependent transactivators affect long-term expression of mouse erythropoietin delivered by a helper-dependent adenoviral vector. *J Gene Med* **7**: 1086–1096.
39. Cordier, L, Gao, GP, Hack, AA, McNally, EM, Wilson, JM, Chirmule, N *et al.* (2001). Muscle-specific promoters may be necessary for adeno-associated virus-mediated gene transfer in the treatment of muscular dystrophies. *Hum Gene Ther* **12**: 205–215.
40. McGee Sanftner, LH, Rendahl, KG, Quiroz, D, Coyne, M, Ladner, M, Manning, WC *et al.* (2001). Recombinant AAV-mediated delivery of a tet-inducible reporter gene to the rat retina. *Mol Ther* **3**: 688–696.
41. Lamartina, S, Silvi, L, Roscilli, G, Casimiro, D, Simon, AJ, Davies, ME *et al.* (2003). Construction of an rtTA2(s)-m2/tts(kid)-based transcription regulatory switch that displays no basal activity, good inducibility, and high responsiveness to doxycycline in mice and non-human primates. *Mol Ther* **7**: 271–280.
42. Srour, MA, Fechner, H, Wang, X, Siemetzki, U, Albert, T, Oldenburg, J *et al.* (2003). Regulation of human factor IX expression using doxycycline-inducible gene expression system. *Thromb Haemost* **90**: 398–405.
43. Kistner, A, Gossen, M, Zimmermann, F, Jerecic, J, Ullmer, C, Lubbert, H *et al.* (1996). Doxycycline-mediated quantitative and tissue-specific control of gene expression in transgenic mice. *Proc Natl Acad Sci USA* **93**: 10933–10938.
44. Knott, A, Garke, K, Urlinger, S, Guthmann, J, Muller, Y, Thellmann, M *et al.* (2002). Tetracycline-dependent gene regulation: combinations of transregulators yield a variety of expression windows. *Biotechniques* **32**: 796, 798, 800 passim.
45. Rendahl, KG, Quiroz, D, Ladner, M, Coyne, M, Seltzer, J, Manning, WC *et al.* (2002). Tightly regulated long-term erythropoietin expression in vivo using tet-inducible recombinant adeno-associated viral vectors. *Hum Gene Ther* **13**: 335–342.
46. Salucci, V, Scarito, A, Aurisicchio, L, Lamartina, S, Nicolaus, G, Giampaoli, S *et al.* (2002). Tight control of gene expression by a helper-dependent adenovirus vector carrying the rtTA2(s)-M2 tetracycline transactivator and repressor system. *Gene Ther* **9**: 1415–1421.
47. Wang, L, Muramatsu, S, Lu, Y, Ikeguchi, K, Fujimoto, K, Okada, T *et al.* (2002). Delayed delivery of AAV-GDNF prevents nigral neurodegeneration and promotes functional recovery in a rat model of Parkinson's disease. *Gene Ther* **9**: 381–389.
48. Okada, T, Uchibori, R, Iwata-Okada, M, Takahashi, M, Nomoto, T, Nonaka-Sarukawa, M *et al.* (2006). A histone deacetylase inhibitor enhances recombinant adeno-associated virus-mediated gene expression in tumor cells. *Mol Ther* **13**: 738–746.
49. Okada, T, Nomoto, T, Yoshioka, T, Nonaka-Sarukawa, M, Ito, T, Ogura, T *et al.* (2005). Large-scale production of recombinant viruses by use of a large culture vessel with active gassing. *Hum Gene Ther* **16**: 1212–1218.
50. Okada, T, Mizukami, H, Urabe, M, Nomoto, T, Matsushita, T, Hanazono, Y *et al.* (2001). Development and characterization of an antisense-mediated prepackaging cell line for adeno-associated virus vector production. *Biochem Biophys Res Commun* **288**: 62–68.

Gene Therapy (2009) 16, 383–391

www.nature.com/gt

ORIGINAL ARTICLE

Systemic delivery of IL-10 by an AAV vector prevents vascular remodeling and end-organ damage in stroke-prone spontaneously hypertensive rat

T Nomoto[1,2], T Okada[1,3], K Shimazaki[4], T Yoshioka[1], M Nonaka-Sarukawa[1], T Ito[1], K Takeuchi[5], K-i Katsura[2], H Mizukami[1], A Kume[1], S Ookawara[5], U Ikeda[6], Y Katayama[2] and K Ozawa[1]

[1]Division of Genetic Therapeutics, Center for Molecular Medicine, Jichi Medical University, Tochigi, Japan; [2]Second Department of Internal Medicine, Nippon Medical School, Tokyo, Japan; [3]Department of Molecular Therapy, National Institute of Neuroscience, National Center of Neurology and Psychiatry, Tokyo, Japan; [4]Department of Physiology, Jichi Medical University, Tochigi, Japan; [5]Department of Anatomy, Jichi Medical University, Tochigi, Japan and [6]Department of Cardiovascular Medicine, Shinshu University Graduate School of Medicine, Nagano, Japan

Interleukin-10 (IL-10) ameliorates various T-helper type 1 cell-mediated chronic inflammatory diseases. Although the therapeutic benefits of IL-10 include antiatherosclerotic effects, pathophysiological effects of IL-10 on vascular remodeling in hypertension have not yet been elucidated. These studies were designed to determine whether sustained IL-10 expression, mediated by an adeno-associated virus (AAV) vector, prevents vascular remodeling and target-organ damage in the stroke-prone spontaneously hypertensive rat (SHR-SP)—an animal model of malignant hypertension. A single intramuscular injection of an AAV1 vector encoding rat IL-10 introduced long-term IL-10 expression. These IL-10-transduced rats had decreased stroke episodes and proteinuria, resulting in improved survival. Histological examination revealed a reduced level of deleterious vascular remodeling of resistance vessels in the brain and kidney of these rats. Immunohistochemical analysis indicated that IL-10 inhibited the enhanced renal transforming growth factor-β expression and perivascular infiltration of monocytes/macrophages and nuclear factor-κB-positive cells normally observed in the SHR-SP. Four weeks after IL-10 vector injection, systolic blood pressure significantly decreased and this effect persisted for several months. Overall, AAV vector-mediated systemic IL-10 expression prevented vascular remodeling and inflammatory lesions of target organs in the SHR-SP. This approach provides significant insights into the prevention strategy of disease onset with unknown genetic predisposition or intractable polygenic disorders.

Gene Therapy (2009) **16,** 383–391; doi:10.1038/gt.2008.151; published online 25 September 2008

Keywords: *IL-10; AAV vector; vascular remodeling; stroke; hypertension; SHR-SP*

Introduction

Interleukin-10 (IL-10), a pleiotropic cytokine produced by type-2 helper T (Th) cells, regulates inflammatory reactions. Specifically, it inhibits macrophage activation, T-cell proliferation and proinflammatory cytokine production, including the release of interferon (IFN)-γ, IL-2 and tumor necrosis factor-β from Th type 1 (Th1) cells.[1,2] The importance of inflammation in the pathogenesis of atherosclerosis has been increasingly acknowledged.[3] Recent studies have shown that IL-10 decreases atherosclerotic lesions in the large vessels through an anti-inflammatory mechanism.[4–6] We also reported that in ApoE-deficient mice, a single intramuscular adeno-associated virus (AAV) vector injection resulted in sustained IL-10 expression for over 6 months and improved atherosclerosis.[7]

Correspondence: Dr K Ozawa or Dr T Okada, Division of Genetic Therapeutics, Center for Molecular Medicine, Jichi Medical University, 3311-1 Yakushiji, Shimotsuke, Tochigi 329-0498, Japan.
E-mail: kozawa@jichi.ac.jp or t-okada@ncnp.go.jp
Received 22 May 2008; revised 31 July 2008; accepted 1 August 2008; published online 25 September 2008

Several evidences suggest that IL-10 regulates endothelial NOS, endothelin-1 and heme oxygenase-1 that substantially associate with blood pressure and vascular remodeling of resistance artery in a genetic model of hypertension. Although the overall contribution of inflammation to vascular damage in patients with hypertension remains to be clarified, several forms of experimental hypertension have been used to demonstrate monocyte/macrophage infiltration into the vessels of target organs, such as the brain and kidney.[8,9] Circulating monocytes are activated in hypertensive patients,[10] and mechanically stretched human monocytic cells induce expression of inflammation-related genes.[11] The spontaneously hypertensive rat (SHR) and its stroke-prone substrain, the stroke-prone spontaneously hypertensive rat (SHR-SP), are well-characterized models of genetic hypertension that mimic human essential hypertension.[12] Recent evidence indicates that an inflammatory reaction may underlie the pathogenesis of arteriolosclerosis in the SHR.[13,14] As a consequence, the role of inflammation in vascular remodeling associated with hypertension-induced organ damage is being researched avidly. However, the role of IL-10 in regulating

vascular remodeling of resistance vessels remains to be clarified.

Adenoviral vectors can efficiently deliver genes to a wide variety of dividing and non-dividing cell types. However, one drawback with their use is that immunological elimination of infected cells often results in transient gene expression *in vivo*.[15] AAV vectors can efficiently transduce non-dividing skeletal muscle cells and achieve sustained expression of therapeutic genes with minimum inflammatory and immune responses.[16] The transduced muscle cells produce therapeutic proteins, which are secreted into the systemic circulation.

In this study, we hypothesized that an IL-10-mediated anti-inflammatory approach could also retard the progression of vascular remodeling in resistance artery. Here, we demonstrate that AAV-mediated sustained IL-10 expression prevents structural change in resistance artery and peripheral organ damage in the SHR-SP model.

Results

Expression of rat IL-10 in vitro *and* in vivo

To confirm the expression of AAV1RIL10 *in vitro*, total cell lysates of human embryonic kidney 293 (HEK293) cells transduced with recombinant AAV (rAAV), and the corresponding conditioned media, were prepared for western blot analysis of rat IL-10. IL-10 was detected in the conditioned medium of HEK293 cells transduced with AAV1RIL10, but not in the AAV1RIL10 cell lysate or the conditioned medium of HEK293 cells transduced with AAV1LacZ (Figure 1a). These results indicate that IL-10 is secreted from transduced cells. The biological activity of rat IL-10 was confirmed using lipopolysaccharide-stimulated rat splenocytes *in vitro*. After stimulation with lipopolysaccharide, splenocytes were incubated with the conditioned medium of HEK293 cells transduced with AAV1RIL10 or AAV1LacZ. Production of IFN-γ was suppressed by incubation with AAV1RIL10 but not with AAV1LacZ (data not shown), suggesting that rat IL-10 produced by AAV1RIL10 was biologically active. The serum IL-10 concentration in the SHR-SP transduced with rAAV vectors is shown in Figure 1b. Three weeks after gene delivery, serum IL-10 was elevated in a dose-dependent manner and this remained stable over a 6-month period.

Stroke-free duration and neurological score of SHR-SP

To analyze whether stable expression of IL-10 can modify the frequency of stroke episodes in the SHR-SP, the incidences of stroke-associated symptoms were observed (Figure 2a). Although all control rats (injected with AAV1LacZ or saline) showed stroke-associated symptoms, no stroke-associated symptoms were observed in the rats transduced with AAV1RIL10 (1×10^{11} or 1×10^{12} genome copies per body (g.c. per body)), even more than 7 months after gene delivery. As the SHR-SP stroke episodes are usually temporary and associated neurological deficits fluctuate significantly at an early stage, the SHR-SP neurological score was determined 6 months after gene delivery. As shown in Figure 2b, control rats revealed marked deterioration, whereas rats transduced

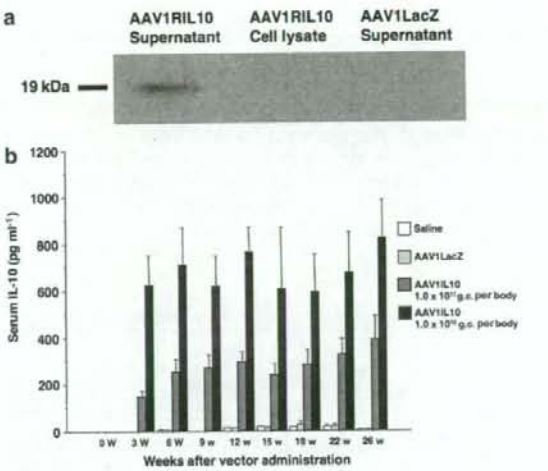

Figure 1 Long-term rAAV-mediated expression of rat IL-10 *in vivo*. (**a**) Expression of rat IL-10 in HEK293 cells. Total cell lysates of HEK293 cells were transduced with rAAVs, and the corresponding conditioned medium was probed with an antibody against rat IL-10. Rat IL-10 was detectable in conditioned medium (lane 1) of HEK293 cells transduced with AAV1RIL10 at 1×10^4 g.c. per cell but not in the corresponding cell lysate (lane 2). It was also undetectable in conditioned medium of HEK293 cells transduced with AAV1-LacZ (lane 3). (**b**) Serum IL-10 concentration in the SHR-SP. AAV1RIL10 (1×10^{11} or 1×10^{12} g.c. per body), AAV1LacZ (1×10^{11} g.c. per body) or saline was injected into the bilateral anterior tibial muscles of the male SHR-SP at 6 weeks of age. Serum concentration of rat IL-10 was measured periodically by ELISA after gene delivery. Values represent mean ± s.d. ($n = 5$ for each group). ELISA, enzyme-linked immunosorbent assay; g.c., genome copies; IL, interleukin; rAAV, recombinant AAV; SHR-SP, stroke-prone spontaneously hypertensive rat.

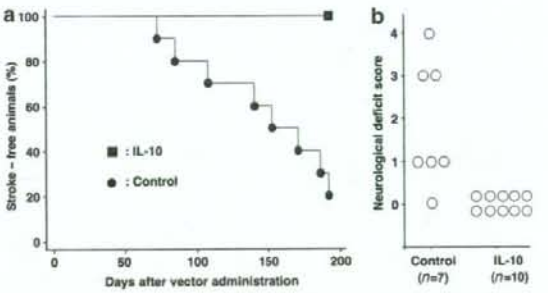

Figure 2 Prevention of stroke episodes in the IL-10-transduced SHR-SP. (**a**) Stroke-free duration of SHR-SP. Male SHR-SP were injected with AAV1RIL10 (IL-10, 1×10^{11} or 1×10^{12} g.c. per body, $n = 5$ each), AAV1LacZ (1×10^{11} g.c. per body, $n = 5$) or saline ($n = 5$) in the bilateral anterior tibial muscles at 6 weeks of age. Control group is comprised of the AAV1LacZ-injected animals and saline-injected animals. Seizure, paralysis of hindlimb, as well as decreased activity, were all regarded as symptoms. Rats were behaviorally assessed every day. The percentage of stroke-free animals was analyzed by the Kaplan–Meier method. The AAV1-RIL10-treated group showed significantly prolonged stroke-free duration compared with the control group ($P < 0.001$). (**b**) Neurological deficit scores of SHR-SP. Six months after gene delivery, neurological deficits were evaluated according to a scoring system described in the Materials and methods section. $P < 0.005$ vs control group. g.c., genome copies; IL, interleukin; SHR-SP, stroke-prone spontaneously hypertensive rat.

with the AAV1RIL10 (1×10^{11} or 1×10^{12} g.c. per body) showed no neurological deficits at this time point.

Histological evaluation and immunohistochemical examination of the cerebral parenchyma

Representative morphological changes and immunohistochemical analysis in the cerebral parenchyma are shown in Figure 3. Multiple ischemic foci (Figure 3a) and hyalinotic changes of the arterioles with perivascular cystic change (Figure 3c) were observed in the vehicle-treated group 7 months after gene delivery. In the AAV1RIL10-treated group, arteriolosclerosis and ischemic foci were negligible across the whole brain at the same time point (Figures 3b and d). Seven months after gene delivery, marked infiltration of ED1-positive (Figure 3e) or CD11b-positive cells (Figure 3g) was observed around the pial arterioles of the cerebral parenchyma in the vehicle-treated group. In the AAV1-RIL10-treated group, infiltration of ED1-positive (Figure 3f) or CD11b-positive cells (Figure 3h) in the pial arterioles was rare. Immunoreactivity of collagen type IV on the vessel walls was also higher in the control brain than in the AAV1RIL10-treated brain (Figures 3i and j).

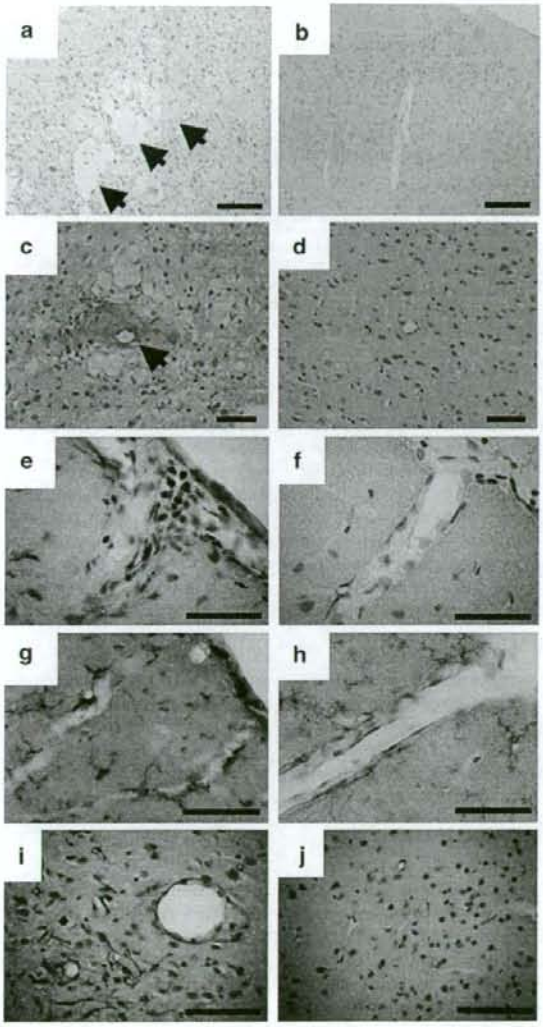

Figure 3 Morphological changes and immunohistochemical examination in the cerebral parenchyma. SHR-SP was transduced with AAV1LacZ (**a**, **c**, **e**, **g** and **i**) or AAV1RIL10 (**b**, **d**, **f**, **h** and **j**). Morphological changes were evaluated by hematoxylin and eosin (HE; **a** and **b**) and periodic acid Schiff stain (PAS; **c** and **d**) at 7 months after gene delivery. Scale bars: 100 μm (**a** and **c**) and 50 μm (**b** and **d**). Representative immunohistochemical examination of the brain at 7 months after gene delivery (**e**–**j**). Immunohistochemical analysis of cells expressing ED1 (**e** and **f**) or CD11b (**g** and **h**) or collagen type IV (**i** and **j**) in the cerebral parenchyma of the transduced animals. Scale bars: 100 μm (**e**–**j**). SHR-SP, stroke-prone spontaneously hypertensive rat.

Protected renal function in SHR-SP

To assess the progression of renal damage, urine was collected over a 24-hour period from rats housed in metabolic cages at 8, 12, 16 and 24 weeks after gene delivery and proteinuria was evaluated. Although the vehicle-treated group showed a significant increase in proteinuria with age, in the AAV1RIL10-transduced group, proteinuria remained low (Figures 4a). Representative morphological changes in the kidney at 7 months after gene delivery are shown in Figures 4b–e. The vehicle-treated group had major cortical damage including decreased cell height, loss of brush borders in the proximal tubules, sclerotic glomeruli, accumulated colloid or protein casts and focal accumulation of inflammatory cells (Figure 4b). Arteriolar fibrinoid necrosis was also apparent in the vehicle-treated group (Figure 4c). However, in the AAV1RIL10-transduced group, normal kidney structure was preserved (Figure 4d) and arteriolar fibrinoid necrosis was rarely seen (Figure 4e) at 7 months after gene delivery.

Immunohistochemical examination of the kidney

Representative immunohistochemical examination of the kidney at 7 months after gene delivery is shown in Figure 5. Marked infiltration of ED1-positive cells was observed in the small arteries of the control group (Figure 5a) compared with the AAV1RIL10-treated group (Figure 5b). Intense transforming growth factor (TGF)-β immunoreactivity in proximal tubular epithelial cells was also evident in the vehicle-treated group (Figure 5c) compared with the AAV1RIL10-treated group (Figure 5d). Infiltration of nuclear factor (NF)-κB p65 subunit-positive cells was also detected in the small arteries (Figures 5e and f) and proximal tubules (Figures 5g and h) in the control group. In contrast, infiltration of NF-κB p65 subunit-positive cells in either the vessel wall (Figure 5i) or interstitium (Figure 5j) was barely detectable in the AAV1RIL10-treated group.

Serum biochemistry

Aspartate aminotransferase (AST), alanine aminotransferase (ALT), total cholesterol, blood urea nitrogen and creatinine significantly decreased in the AAV1RIL10-treated group at 6 months after transduction (Table 1). Serum albumin, glucose and triglyceride were significantly decreased in the control group. Serum cytokine concentration profile is also summarized in Table 1. IFN-γ and TGF-β concentrations significantly decreased in the AAV1RIL10-treated group at 6 weeks after transduction.

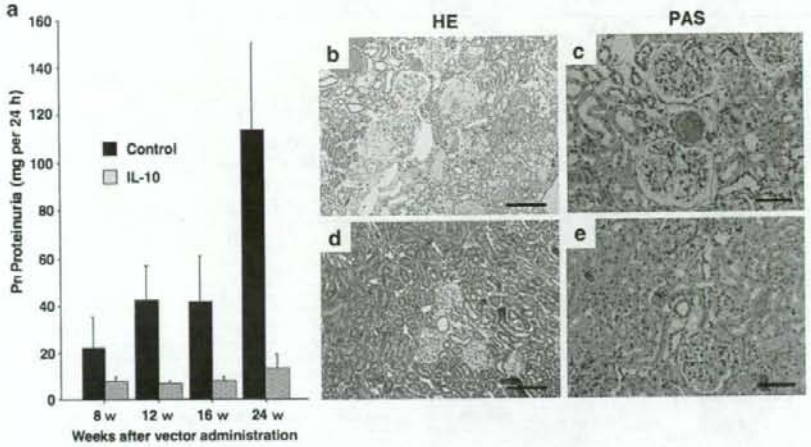

Figure 4 Prevention of renal dysfunction in the IL-10-transduced SHR-SP. (**a**) Reduction of proteinuria in SHR-SP. The transduction protocol is identical to that used in Figure 2. Urine was collected from rats in metabolic cages for a 24-hour period at 8, 12, 16 and 24 weeks after gene delivery and then proteinuria was evaluated. SHR-SP transduced with AAV1RIL10 showed a significant reduction in proteinuria ($P<0.001$, $n=10$ for each group). Data are shown as mean ± s.d. Representative morphological changes in the kidney of SHR-SP transduced with AAV1LacZ (**b** and **c**) or AAV1RIL10 (**d** and **e**) were evaluated by hematoxylin and eosin (HE; **b** and **d**) and periodic acid Schiff stain (PAS; **c** and **e**) at 7 months after gene delivery. Scale bars: 100 μm (**b** and **d**) and 50 μm (**c** and **e**). IL, interleukin; SHR-SP, stroke-prone spontaneously hypertensive rat.

Blood pressure of SHR-SP and morphological changes in the carotid artery

Systolic blood pressure of the SHR-SP is shown in Figure 6. At 6 weeks of age, systolic blood pressure in the control and AAV1RIL10-treated groups was equivalent. Blood pressure gradually increased with age in the control group and reached a plateau of approximately 210–230 mm Hg at 16 weeks of age. Interestingly, systolic blood pressure in the AAV1RIL10-transduced group plateaued at lower values than controls. This effect on the systolic blood pressure persisted over 30 weeks after transduction (Figure 6a). A significant correlation was observed between serum IL-10 concentration and systolic blood pressure at 9 weeks after transduction (Figure 6b). Histological changes in the carotid artery 6 months after vector administration are summarized in Figure 6c. Compared with the control group, carotid artery integrity was well preserved in the AAV1RIL10-treated group. Quantitative analysis of carotid diameter and media thickness is shown in Figure 6d. Both of these parameters decreased significantly in the AAV1RIL10-treated group.

Prolonged survival of SHR-SP

Survival of SHR-SP transduced with AAV1RIL10 (1×10^{11} or 1×10^{12} g.c. per body), AAV1LacZ or saline was evaluated by Kaplan–Meier survival analysis (Figure 7). Transduction of the SHR-SP with AAV1RIL10 significantly prolonged survival compared with that of controls (AAV1LacZ or saline; $n=10$ for each group; $P<0.001$).

Discussion

Here we demonstrate that sustained IL-10 expression can prevent the progression of arteriolosclerosis and associated target-organ damage in the SHR-SP. A single intramuscular injection of an AAV1-based vector encoding IL-10 achieved long-term systemic IL-10 expression. The resultant IL-10-transduced rats showed an improvement in proteinuria, as well as prolonged stroke-free duration and survival. Histological examination revealed a reduction in brain arteriolosclerosis and nephrosclerosis when compared with control rats. Immunohistochemical examination confirmed decreased infiltration of monocytes/macrophages and NF-κB-positive cells in the brain and renal arteriolosclerotic lesions of these rats. IL-10-transduced rats also exhibited a sustained decrease in the systolic blood pressure compared with controls.

The AAV vector, derived from a non-pathogenic parvovirus, can transduce non-dividing neuronal and skeletal muscle cells, and can also achieve long-term transgene expression *in vivo* with minimal inflammatory and immune responses.[17,18] Intramuscular injection of the vector is used to transduce the skeletal muscle *in vivo* and the resultant transduced muscle cells produce the encoded proteins, which are secreted into the systemic circulation. Preclinical and clinical investigations using AAV2-based vectors have demonstrated efficient neuronal transduction and therapeutic benefits in neurodegenerative diseases with minimum adverse effects.[18] However, the application of this technique might be limited because of insufficient levels of transgene expression in other tissues.[19] The AAV serotype 1-based vector has distinct receptors that may promote the initial viral binding and entry into muscle cells, leading to a more efficient transduction to skeletal muscle than AAV2-based vectors.[20] We therefore utilized an AAV1-pseudotyped vector in this study. We confirmed the presence of sustained and adequate IL-10 serum levels in SHR-SP after a single intramuscular injection of AAV1IL10.

We initially evaluated the effects of IL-10 on SHR-SP behavior. IL-10-tranduced rats showed decreased stroke-associated symptoms compared with the untreated controls. This behavioral improvement might be

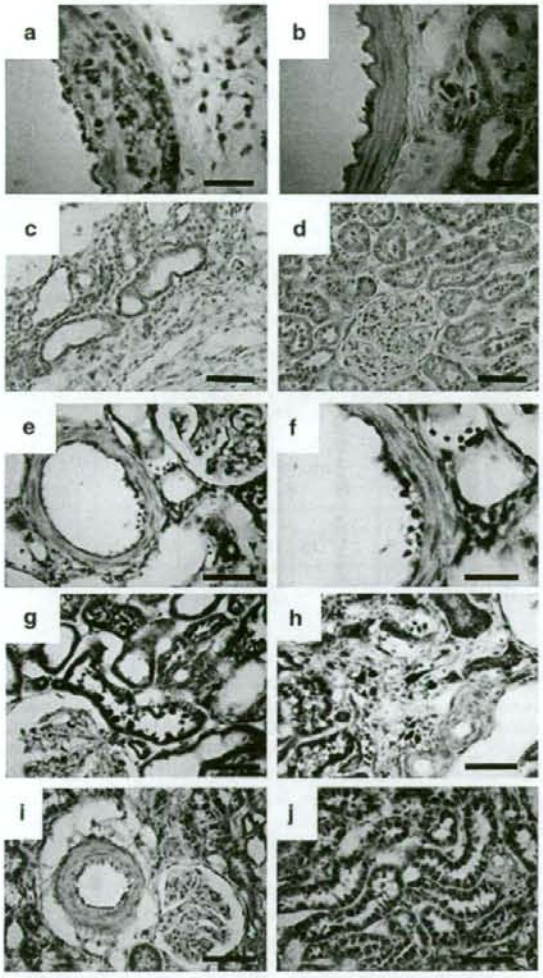

Figure 5 Immunohistochemical examination of the kidney at 7 months after gene delivery. Immunohistochemical detection of cells expressing ED1 (**a** and **b**) or TGF-β (**c** and **d**) or NF-κB p65 subunit (**e**–**j**) in the kidney of the SHR-SP transduced with AAV1LacZ (**a**, **c**, **e**, **f**, **g** and **h**) or AAV1RIL10 (**b**, **d**, **i** and **j**). Scale bars: 30 μm (**a**, **b** and **f**) and 50 μm (**c**–**e** and **g**–**j**). NF-κB, nuclear factor-κB; SHR-SP, stroke-prone spontaneously hypertensive rat; TGF-β, transforming growth factor-β.

explained by IL-10-mediated vasculoprotection, although demonstrating direct neuroprotective effects of IL-10 would require further experimentation. Our results indicate that the vasculoprotective effects of IL-10 might be associated with its anti-inflammatory properties. Accumulating evidence supports the notion that hypertension is the biggest risk factor for brain lacunar syndrome and intracerebral hemorrhage, suggesting that high blood pressure affects the local injury of intracerebral arteries.[21] Degenerative vascular changes, similar to those seen in human essential hypertensives, occur in the brain of the SHR and SHR-SP.[22] We demonstrated that long-term systemic IL-10 expression prevented the arteriolosclerotic lesions, normally characterized by

Table 1 Serum biochemical analysis of AAV-transduced SHR-SP

	Control (n = 9)	*IL-10* (n = 10)
AST	57.8 ± 13.1	35.5 ± 6.2***
ALT	89.5 ± 8.0	59.0 ± 17.0**
Albumin	3.9 ± 0.2	4.7 ± 0.1***
Total cholesterol	107.1 ± 22.5	64.2 ± 3.2***
Triglyceride	57.3 ± 39.4	69.3 ± 12.6*
Glucose (fasting)	117.6 ± 9.7	145.1 ± 13.2***
Blood urea nitrogen	28.8 ± 7.0	17.8 ± 2.1**
Creatinine	0.37 ± 0.06	0.22 ± 0.01***
	Control (n = 10)	*IL-10* (n = 10)
IFN-γ	2.88 ± 1.02	1.59 ± 0.45††
TGF-β	18.0 ± 2.6	15.1 ± 2.6†

Abbreviations: AAV, adeno-associated virus; SHR-SP, stroke-prone spontaneously hypertensive rat.
The transduction protocol is identical to that used in Figure 2. Serum biochemical analysis of the SHR-SP was performed at 6 months after injection. Serum cytokine profile in the AAV1RIL10-transduced SHR-SP (IL-10) or saline-treated SHR-SP (control) was also analyzed at 6 weeks after injection. Each value is the mean ± s.d.
*$P<0.01$, **$P<0.005$, ***$P<0.001$, versus control SHR-SP.
†$P<0.05$, ††$P<0.005$, versus control SHR-SP.

fibrinoid necrosis and monocyte/macrophage infiltration, in cerebral arteries of the SHR-SP. We also observed reduced serum levels of IFN-γ, a proinflammatory cytokine released by Th1 cells, in the IL-10-transduced rats. A Th1-dominant T-cell population is associated with progression of hypertensive organ damage.[17] However, IL-10 is reported to deactivate monocytes by reducing IFN-γ production,[23] thereby improving atherosclerotic lesions by shifting the Th pattern from Th1-dominant to Th2-dominant. These observations suggest that IL-10 might regulate vascular inflammation by modulating Th imbalance. In addition, IL-10 inhibits the expression of adhesion molecules and matrix metalloproteinases, as well as smooth muscle cell proliferation.[24–28] These IL-10 effects might regulate local vascular inflammation and remodeling, also leading to an improvement in arteriolosclerosis. Clearly, further investigations are required to clarify the mechanism(s) by which IL-10 improves hypertension-associated vascular damage in more detail.

In this study, we also observed that activated NF-κB-positive cells accumulate in renal arteriolosclerotic lesions of the SHR-SP. The transcription factor, NF-κB, is activated by a wide variety of proinflammatory molecules, such as IL-8, macrophage chemotactic protein-1, intercellular adhesion molecule-1, vascular-cell adhesion molecule-1 and E-selectin.[29–31] Monocyte infiltration into the small renal arteries stimulates NF-κB activation, leading to chemokine and cytokine expression in the kidney. NF-κB is also known to be activated in the course of vascular inflammation and renal injury in the SHR.[32] In contrast, IL-10 directly inhibits NF-κB activation in macrophages.[33] In this study, IL-10-transduced rats showed a decrease in activated NF-κB-positive cells in the renal arteriolosclerotic lesions of SHR-SP, which might reflect reduced inflammatory activity within these lesions.